Fakultät für Medizin

Urologische Klinik und Poliklinik

Functional genomics identifies multiple clinically actionable resistance mechanisms to CDK4/6 inhibition in bladder cancer

Zhichao Tong

Vollständiger Abdruck der von der Fakultät für Medizin der Technischen Universität München zur Erlangung des akademischen Grades eines

Doktors der Medizin

genehmigten Dissertation

Vorsitzende/r: Prof. Dr. Jürgen Schlegel

Prüfer der Dissertation:

1: Prof. Dr. Jürgen E. Gschwend

2: Prof. Dr. Dieter Saur

Die Dissertation wurde am 22.11.2018 bei der Fakultät für Medizin der Technischen Universität München eingereicht und durch die Fakultät für Medizin am 16.04.2019 angenommen

AFFIDAVIT

I hereby declare that the dissertation titled

Functional genomics identifies multiple clinical actional resistance mechanisms to CDK4/6 inhibition in bladder cancer prepared under the guidance and supervision of Univ.-Prof. Dr. Jürgen E. Gschwend at the Department of Urology

and submitted to the degree-awarding institution of: The Faculty of Medicine of TUM is my own, original work undertaken in partial fulfillment of the requirements for the doctoral degree. I have made no use of sources, materials or assistance other than those specified in § 6 (6) and (7), clause 2.

[X] I have not employed the services of an organization that provides dissertation supervisors in return for payment or that fulfills, in whole or in part, the obligations incumbent on me in connection with my dissertation.

[X] I have not submitted the dissertation, either in the present or a similar form, as part of another examination process.

 [ ] The complete dissertation was published in

the degree-awarding institution:

has approved prior publication of the dissertation.

[X] I have not yet been awarded the desired doctoral degree nor have I failed the last possible attempt to obtain the desired degree in a previous doctoral program.

[ ] I have already applied for admission to a doctoral program at the school or college of
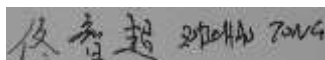

at (university)

by submitting a dissertation on the topic

With the result:

I am familiar with the publicly available Regulations of the Award of Doctoral Degrees of TUM, in particular § 28 (Invalidation of doctoral degree) and § 29 (Revocation of doctoral degree). I am aware of the consequences of filling a false affidavit.

[X] I agree   [ ] I do not agree

that my personal data is stored in the TUM alumni database. Munich, 11.11.2018

Munich, 11.11.2018

Abstract

Though CDK4/6 inhibition has already been proven as a promising approach for the treatment of bladder cancer in preclinical research. However, mechanisms of resistance still are unclear. Therefore, a genome-scale CRISPR-dCas9 gain of function screen for the CDK4/6 inhibitor Palbociclib was performed in the bladder cancer derived cell line T24. Enrichment of sgRNAs were detected using NGS and statistically significant sgDNAs from the screen were analyzed using MAGeCK-VISPR. 1024 sgRNAs encoding for 995 genes were significantly enriched in the screen. In order to validate these data, 8 randomly chosen sgRNAs within the first most significant 500 sgRNAs were functionally validated on a molecular and functional level for mediating resistance to Palbociclib treatment. Comparison of the screen hits to signaling pathways and clinically relevant molecular alterations was performed using DAVID, Reactome, DGIdb and and cBioPortal. We identified enriched sgRNAs in RTKs, PI3K-Akt and Ras/MAPK signaling pathways that are also frequently activated in bladder cancer. Combination of Palbociclib with compounds directed against RTKs, PI3K-Akt, Ras/MAPK and STAT pathways revealed beneficial effects in vitro and in vivo xenografts. Since activation of the signalingpathways that confer resistance are largely regulated by RTKs, we engineered cells that by sgRNA induced hyperactivation of KDR or FGFR3 mediated resistance to palbociclib. Interestingly, in these cells the combination of Palbociclib and respective inhibitors acted synergistically and overcame acquired resistance in those tumors. However, the combination of Palbociclib and mTOR inhibitors did not overcome the induced resistance of KDR or FGFR3 expression. In conclusion, identification of resistance mechanisms and rational combinational therapies could be achieved applying a genome scale CRISPR-dCas9 approach in this study.

Acknowledgments

Lastly, I want to thank my family especially my wife Dr. Shan Liang for always encouraging me to pursue my academic goals. All your endless love and unlimited support means a lot. And deep gratitude to my grandparents, I always know they are watching me and protecting me from heaven.

Contents

List of Figures

List of Tables

List of Symbols and Abbreviations

7-AAD	7-aminoactinomycin D
APS	ammonium persulfate
ATM	Ataxia telangiectasia mutated
ATP	Adenosine Triphosphate
ATR	Ataxia Telangiectasia and Rad3 related
BC	bladder cancer
BCA	bicinchoninic acid
BSA	bovine serum albumin
℃	degree Celsius
CaCl2	calcium chloride
CNA	Copy number alterration
CRISPR	clustered regularly interspaced short palindromic repeats
CAM	chicken chorioallantoic membrane
CDK	Cyclin dependent kinases
CDKI	Cyclin dependent kinase inhibitor
cDNA	complementary DNA
CI	combination index
CIP/KIP	CDK interacting protein/Kinase inhibitory protein
CIS	carcinoma in situ
cm	centimeter
CO2	carbon dioxide
CST	Cell Signalling technology
ctrl	control
dCas9	catalytically inactive Cas9
DDR	DNA damage response

DMEM	Dulbecco's Modified Eagle's Medium
DMSO	dimethylsulfoxide
DNA	deoxyribonucleic acid
DTT	dithiothreitol
EDTA	ethylenediaminetetraacetic acid
EGFR	epidermal growth factor receptor
FDR	False discovery rate
FBS	fetal bovine serum
FDA	Food and drug administration
G1	Gap 1
G2	Gap 2
GOF	Gain-of-function
H2O2	hydrogen peroxide
HCl	hydrogen chloride
HG	high-grade
HPV	human papilloma virus
HRP	horseradish peroxidase
INK4	Inhibitor of CDK4
l	litre
LG	low-grade
LOF	Lost-of-function
LFC	Log2 fold change
m	meter
M	mitosis
MDM2	Mouse double minute 2 homolog
MEK	Mitogen-activated protein kinase kinase

mg	milligram
MIBC	muscle invasive bladder cancer
min	minute
ml	millilitre
mM	millimolar
mTOR	the mechanistic target of rapamycin
NaCl	sodium chloride
NaOH	sodium hydroxide
NEAA	non-essential amino acids
ng	nanogram
nm	nanometer
nM	nanomolar
NMIBC	non-muscle invasive bladder cancer
nmol	nanomole
PAGE	polyacrylamide gel electrophoresis
PBS	phosphate buffered saline
PCR	polymerase chain reaction
PD-L1	Programmed death-ligand 1
pH	potentia hydrogenii
PI3K	phosphatidylinositol-4,5-bisphosphate 3-kinase
PUNLMP	papillary urothelial neoplasm of low malignant potential
PVDF	polyvinylidene fluoride
qPCR	quantitative polymerase chain reaction
RAS	Rat sarcoma
RB	Retinoblastoma
RCF	Relative Centrifugal Force

RNA	ribonucleic acid
RPMI	Roswell Park Memorial Institute
RTKs	Receptor tyrosine kinase
s	second
S	synthesis
SAHF	senescence-associated heterochromatin foci
SA-β-Gal	senescence-associated β-Gal
SD	standard deviation
SDS	sodium dodecyl sulfate
siRNA	small interfering RNA
SRB	sulforhodamine B
TBS	Tris buffered saline
TBST	Tris buffered saline with Tween-20
TCGA	The Cancer Genome Atlas
TEMED	tetramethylethylenediamine
Thr	Threonine
TNM	Tumor, Node, Metastasis
Tris	Tris(hydroxymethyl)-aminomethane
TURBT	transurethral resection of the bladder tumor
V	volt
WT	wild type
µg	microgram
µl	microlitre
µm	micrometer
µM	micromolar
µmol	Micromole

1. Introduction

1.1 Bladder cancer

1.1.1 Epidemiology and Aetiology of bladder cancer

Bladder cancer is the 10th most commonly diagnosed cancer worldwide that causes approximately 150600 deaths in 2005 and the number reached to 188000 in 2015 (Mortality & Causes of Death, 2016). According to the recent Global cancer statistic, there were 549,000 new cases diagonosed and 200,000 deaths caused by bladder cancer in 2018. Bladder cancer is more common in men than in women, with respective incidence and mortality rates of 9.6 and 3.2 per 100,000 in men: about 4 times those of women globally (Bray et al., 2018). The most well-established risk factor for bladder cancer is tobacco smoking and it is estimated to account for 50-65% of male cases and 20-30% of female cases. Second to smoking, occupational exposure to chemicals roughly accounts for 20-25% of bladder cancer. Arsenic ingestion, radiotherapy, chronic inflammation and parasite infection etc. also serve as risk factors to bladder cancer. Bladder cancer also exhibits genetic susceptibility, for example the genetic slow acetylator N-acetyltransferase 2 (NAT2) variants and glutathione S-transferase mu 1 (GSTM1)–null genotypes have been identified as risk factors (Sanli et al., 2017). Although men are more likely to develop bladder cancer than women, yet women present with more advanced disease and have worse survival (Burger et al., 2013; Witjes et al., 2014).

1.1.2 Pathologic classification of bladder cancer

The Tumour–Node–Metastasis system (TNM system) is used to stage bladder cancer by describing the extent of invasion. The 1997 International Society of Urological Pathology grading classification was continued to be recommend by the 2016 WHO classification for grading (Figure 1), yet novel modifications on 4th edition need to be considered (Humphrey, Moch, Cubilla, Ulbright, & Reuter, 2016). More than 90% bladder cancers are urothelial carcinoma which originate from the urothelium, the other rarely variant histology types include squamous/glandular differentiation, nested variant, micropapillary bladder cancer, lymphoepithelioma-like carcinoma of the bladder, plasmacytoid urothelial carcinoma, sarcomatoid carcinoma of the bladder, pure squamous cell carcinoma, adenocarcinoma and small cell carcinoma, the outcome of bladder cancer with variant histology is still conflicting (Willis & Kamat,

2015). Tumours that have invaded the detrusor muscle with stage T2 or above are considered as muscle-invasive bladder cancer (MIBC) and are more likely to metastasize to lymph nodes or other organs. Approximately 75% of newly diagnosed patients have non-muscle-invasive bladder cancer (NMIBC) with stage lower than T1 and 25% have MIBC or metastatic disease (Chamie et al., 2015).

NMIBCs recur in 50–70% cases but rarely progress to invasion (10–15%), and five-year survival is about 90%. These patients are monitored by cystoscopy over many years, multiple resections are often applied. Although risk tables provide a prognostic tool, but so far no molecular biomarkers can predict disease progression accurately. MIBCs have less favourable prognosis with five-year survival <50% and commonly progress to metastasis. Treatment has not advanced for several decades, and new approaches to systemic therapy are needed (Knowles & Hurst, 2015) (Smith et al., 2014).
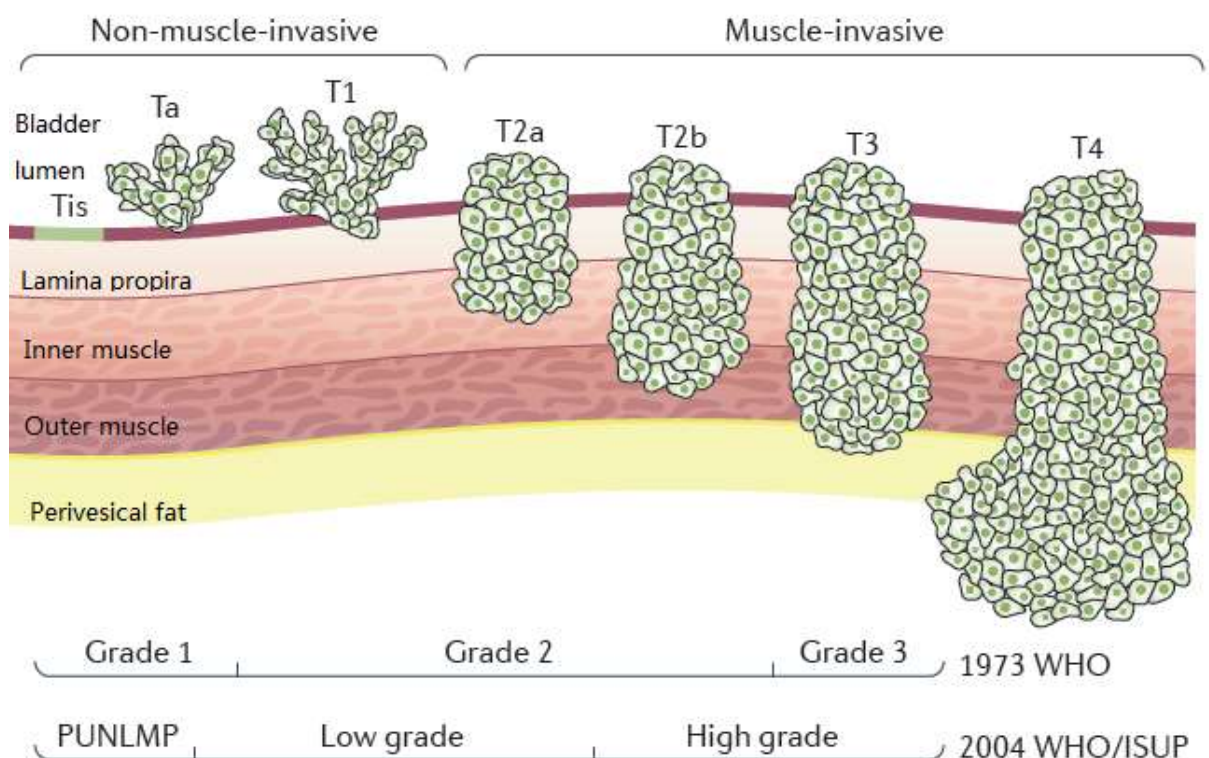
Figure 1: Pathologic types and stages of bladder cancer. TNM staging of bladder cancer is shown. 1973 WHO and 2004 WHO/ISUP, the most important grade differentiation is between low-grade and high-grade tumours is the the greater propensity for invasion (Sanli et al., 2017).

1.1.3 Novel molecular sub-classification of bladder cancer

Although some molecular features have shown association with clinical phenotype, for example, FGFR3 and PIK3CA mutations in low-grade Ta tumors, none of them are currently suitable for application as prognostic biomarkers. High-throughput methodologies of the mRNA, microRNA, protein, epigenetic, and copy number levels offer us a new chance to reveal clinico-pathologic features. A recent comprehensive analysis of 412 muscle-invasive bladder cancers characterized by multiple TCGA analytical platforms suggested more detailed molecular sub-classification based on the multiple platform analyses, and further proposed therapeutic considerations stratified by expression subtyping (Figure 2). Based on the molecular sub-classification, predicting of response and survival after Neoadjuvant Chemotherapy has been achived (Seiler et al., 2017). The other research using a cohort of patients with metastatic urothelial cancer treated with a PD-1 inhibitor, nivolumab demonstrated that in patients with T-cell infiltrated tumors, higher EMT/stroma-related gene expression is associated with lower response rates and shorter progression-free and overall survival(Wang et al., 2018). With more and more available sequencing data from clinic, especially patients with different treatment, we could predict personalized treatment based on exclusive genetic background of patients will be the future direction on treatment of bladder cancer (Chamie et al., 2015; Choi et al., 2014; Dadhania et al., 2016; Guo et al., 2016; Robertson et al., 2018).
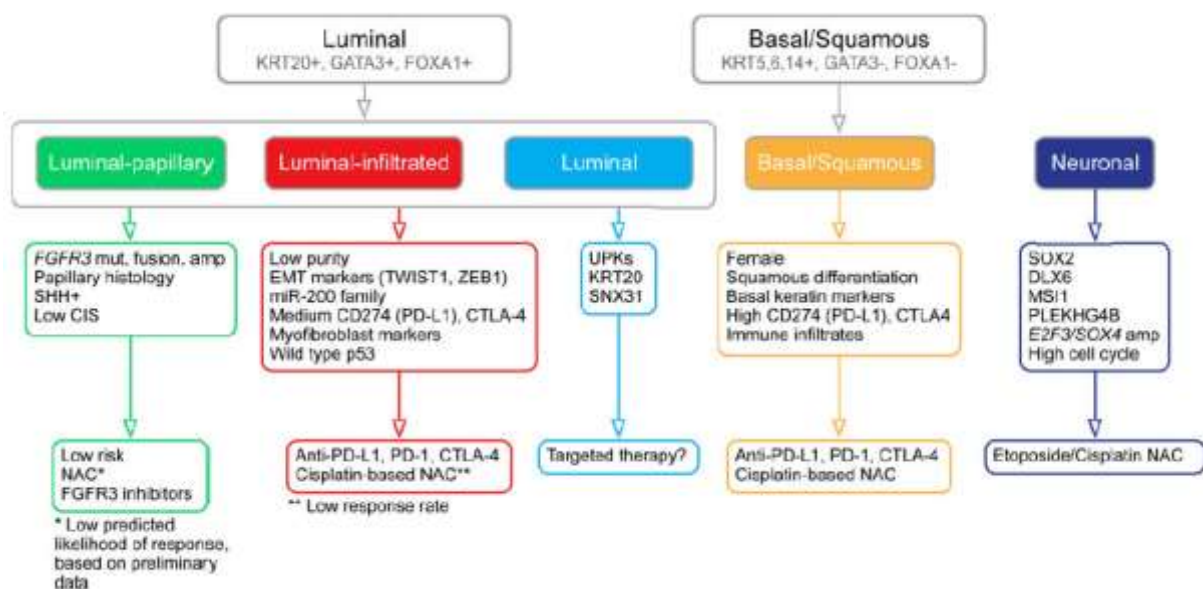
Figure 2: Novel expression-based molecular sub-classification. The key drivers, and proposed treatment strategies for molecular sub-classification (Robertson et al., 2018).

1.1.4 Treatment of bladder cancer

Transurethral resection of bladder tumour (TURBT) is still the first choice when patients diagnosed with NMIBC. Intravesical Bacille-Calmette Guerin (BCG) or MitomycinC therapy are often followed after surgery. BCG immunotherapy is the gold-standard treatment for NMIBC at high risk of recurrence or progression. Though it induces a durable and effective antitumour immune response and results in positive clinical outcomes, there are still a lot of blanks about its mechanism of action. Also, no studies have conclusively demonstrated a concordance among adverse effects, severity, and treatment efficacy (Pettenati & Ingersoll, 2018). When the cancer has invaded the muscle, radical/partial cystectomy and chemotherapy are usually applied (Alfred Witjes et al., 2017; Power & Izawa, 2016). It is encouraging to see novel therapies are developing rapidly for instance immunotherapy, target therapy and gene therapy. However, few therapeutic alternatives have been proven to show satisfactory therapy response in the past years. So far, many target therapies have been tested in bladder cancer, including targeting FGFR, EGFR and VEGFR, yet clinical benefit of these inhibition is unsatisfied. For example, Gefitinib, an orally active selective EGFR inhibitor was evaluated as a single agent in 31 patients with metastatic UC in platinum refractory chemotherapy. 81% of patients demonstrated progressive disease and the median survival time was 3 months(Petrylak et al., 2010). Almost all anti-angiogenic agents as sunitinib, pazopanib, aflibercept and ramucirumab have been evaluated in multiple settings in UC, without clear clinical benefit (Mohammed et al., 2016). These trials failed mostly due to lack of biomarkers. Now checkpoint inhibitors are being explored as potential therapies in bladder cancer. So far several checkpoint targets like PD1, PDL1, and CTLA4 have received the most attention in the treatment of bladder cancer, and have inhibitor agents either approved or in late-stage clinical trials already. The checkpoint inhibitors offer an effective alternative for patients for whom previously there were few options for durable responses, including those who are ineligible for cisplatin-based regimens or who are at risk of significant toxicity(Bellmunt, Powles, & Vogelzang, 2017). It is also promising to combine radiotherapy with checkpoint inhibition to augment the immune response (so-called cytokine storm) triggered by tumor cell death induced by radiotherapy. Hopefully, one can use molecular sub-classification as an effective strategy to identify potential biomarkers for target therapies and achieve patient stratification (Sanli et al., 2017).

1.2 CDK4/6 inhibition

1.2.1 CDK4/6 inhibition in cancer

The CDK4/6-retinoblastoma (RB) pathway regulates the G1-S phase transition in the cell cycle. Mitogenic signaling events, such as the PI3K and MAPK pathways, converge on cyclin D proteins that lead to CDK4/6 pathway activation. Negative control of the CDK4/6-RB pathway is exerted by CDK inhibitors of the Cip-Kip family, including p21 and p27, and the Ink family of proteins, p16Ink4a (encoded by CDKN2A) and p15Ink4b (encoded by CDKN2B). In recent years, a novel class of small molecules which targeting cyclin-dependent kinase 4/6 (CDK4/6) including Palbociclib, Abemaciclib and Ribociclib have been approved by the FDA for treatment of hormone receptor positive breast cancer in combination with hormone therapy (Figure 3) (Iwata, 2018). Abemaciclib alone only led to 19.7% ORR (Dickler et al., 2017), while the combination of Ribociclib and letrozole resulted in a 52.7% and 55.3% ORR (Finn et al., 2016; Hortobagyi et al., 2016), indicating single-agent CDK4/6 inhibitors do not provide long-term anti-tumor effect probably due to de novo resistance and acquired resistance. A Phase II Trial of Palbociclib in Patients with Metastatic Urothelial Cancer After Failure of First-Line Chemotherapy (NCT02334527) just terminated because the first 12 patients have not met endpoint. In this trial, cyclin-dependent kinase inhibitor 2A (CDKN2A) (also referred to as p16) loss and positive Retinoblastoma (Rb) expression were applied as biomarkers which have already been well evaluated in preclinical research, but the results still are unsatisfied. No clear association was observed between alterations in CCND1, CDKN2A, CDKN2B or CCNE1 and treatment response in early exploratory analyses in phase 1 studies in various solid tumors(Infante et al., 2016; Patnaik et al., 2016). So the main challenge is to identify predictive marker that would allow for patient stratification for better response (Guarducci et al., 2017). Hence, even though CDK4/6 inhibitors have been proven to be a promising therapy strategy, stratifying biomarkers for the clinical use of this treatment and improve patient outcomes are urgently needed.
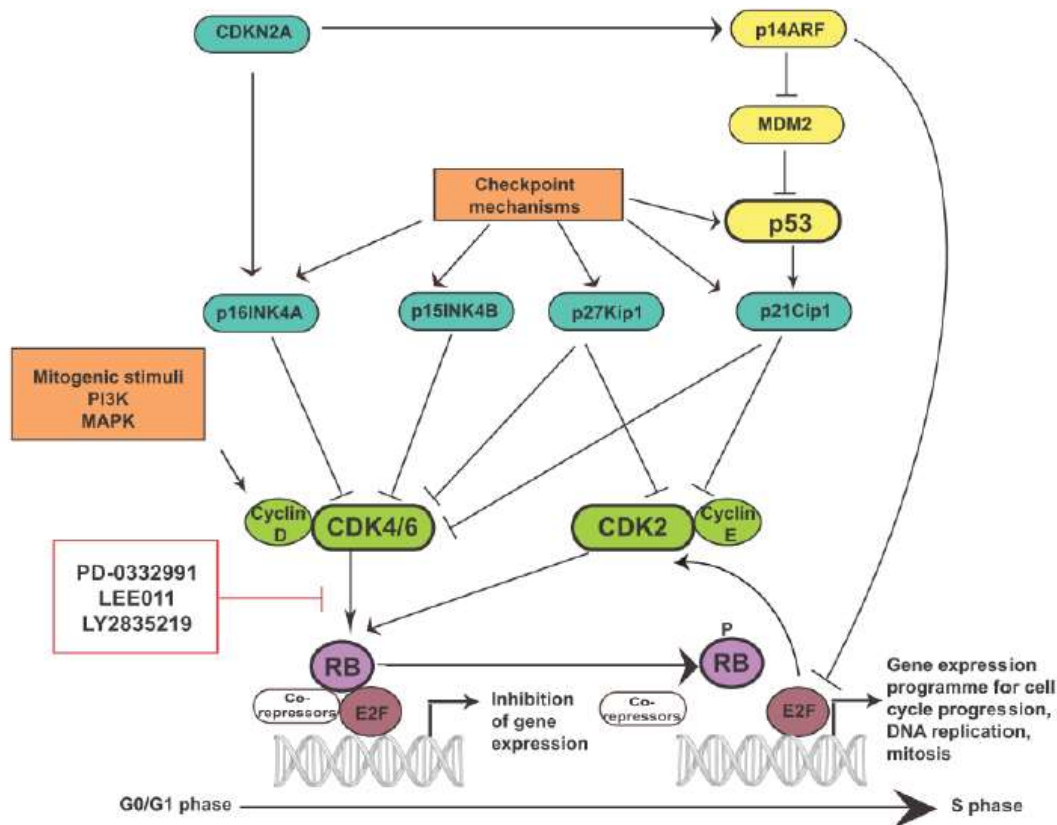
Figure 3: Suggested mechanism of CDK4/6 inhibitors. In a proliferating cell, RB is phosphorylated by CDK4/6-Cyclin D complex under mitogenic stimuli, followed hyperphosphorylation by CDK2-Cyclin E complex. E2Fs may distich and permit the transcription of E2Fs target genes and cell cycle progression from the G1 to the S phase. Activity of CDK4/6 is also regulated via p15/16 and p53 dependent checkpoint. CDK4/6 inhibitors can block activity of CDK4/6 and further arrest cells at G1 phase(Pan et al., 2017).

1.2.2 Preclinical research of applying CDK4/6 inhibitors on bladder cancer

P53/Cell cycle regulation is the most frequently dysregulated pathway in a study of 412 high-grade muscle-invasive urothelial bladder carcinomas on mRNA level (altered in 89% of cases). Thus, targeting the CDK4/6-Rb axis to inhibit cell cycle progression is a rational strategy in bladder cancer. In our previous work, we analyzed the effect of Palbociclib on a panel of bladder cancer cell lines possessing varying genetic alterations in the CDK4/6-RB pathway that resemble those alterations found in primary tumors. Correlating these molecular alterations with the response to the inhibitor demonstrated that cells expressing RB and p16INK4A are the most sensitive to this inhibitor. We also demonstrated that a successful response to

treatment correlates with a reduction in the expression of total RB protein level rather than its phosphorylation status, which might indicate a novel molecular mechanism of regulating progression of the cell cycle. Our results indicate that CDK4/6 inhibition is a promising treatment strategy for bladder cancer and the molecular determinants of treatment response and the development of biomarkers to enable patient stratification are needed for clinical application (Sathe et al., 2016).
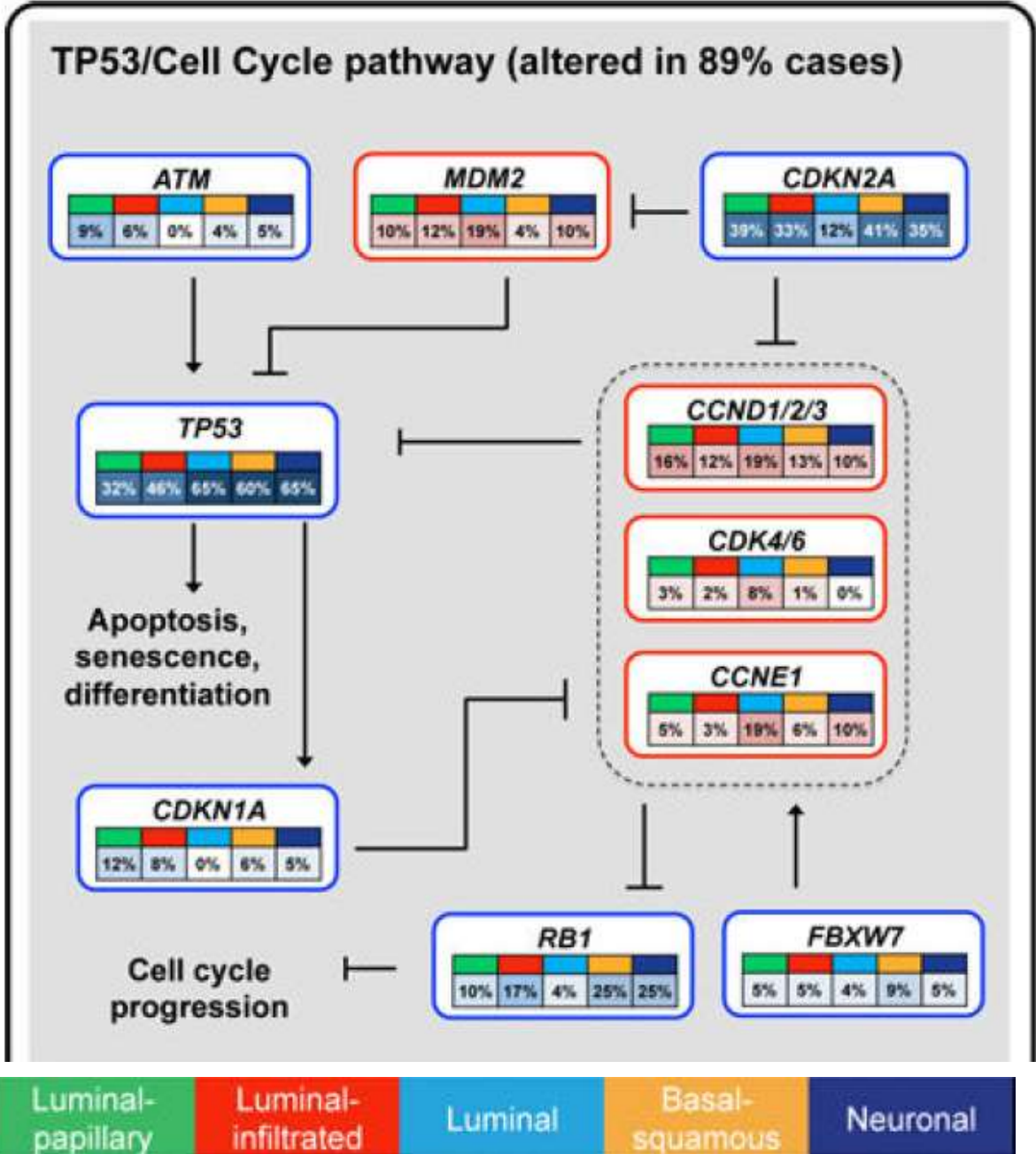
Figure 4: Alteration of p53/Cell Cycle pathway in bladder cancer patients. The p53/Cell Cycle pathway was inactivated in 89% of tumors. Alteration of this pathway is important evidence for molecular sub-classification (Robertson et al., 2018).

1.3 CRISPR technology

1.3.1 Application of CRISPR-Cas9 on inducing GOF and LOF

The RNA-guided CRISPR (clustered regularly interspaced short palindromic repeat)-associated Cas9 nuclease system has emerged in the past years as an alternative powerful tool for both knockout approaches that inactivate genomic loci and strategies that modulate transcriptional activity. When a specific genetic locus contains PAM (protospacer adjacent motif), then the gRNA can recruit the nuclease Cas9 to this site and results in the generation of DNA double strand breaks (DSBs), which are commonly repaired via the NHEJ (non-homologous end joining) DNA repair pathway. Then a generated insertion-deletion (indel) mutation that produces a frameshift, resulting in gene knock down and LOF (loss-of-function). When this system is used for the activation of gene transcription which will lead to GOF (gain-of-function), the Cas9 enzyme is engineered to be catalytically inactive (dCas9) and fused with transcriptional activators such as VP64. This complex is then recruited to regions up- stream of the transcription start site (TSS) of the gene of interest by a complementary gRNA, resulting in increased gene expression (Figure 5) (Doudna & Charpentier, 2014; Gilbert et al., 2014; Shalem, Sanjana, & Zhang, 2015).
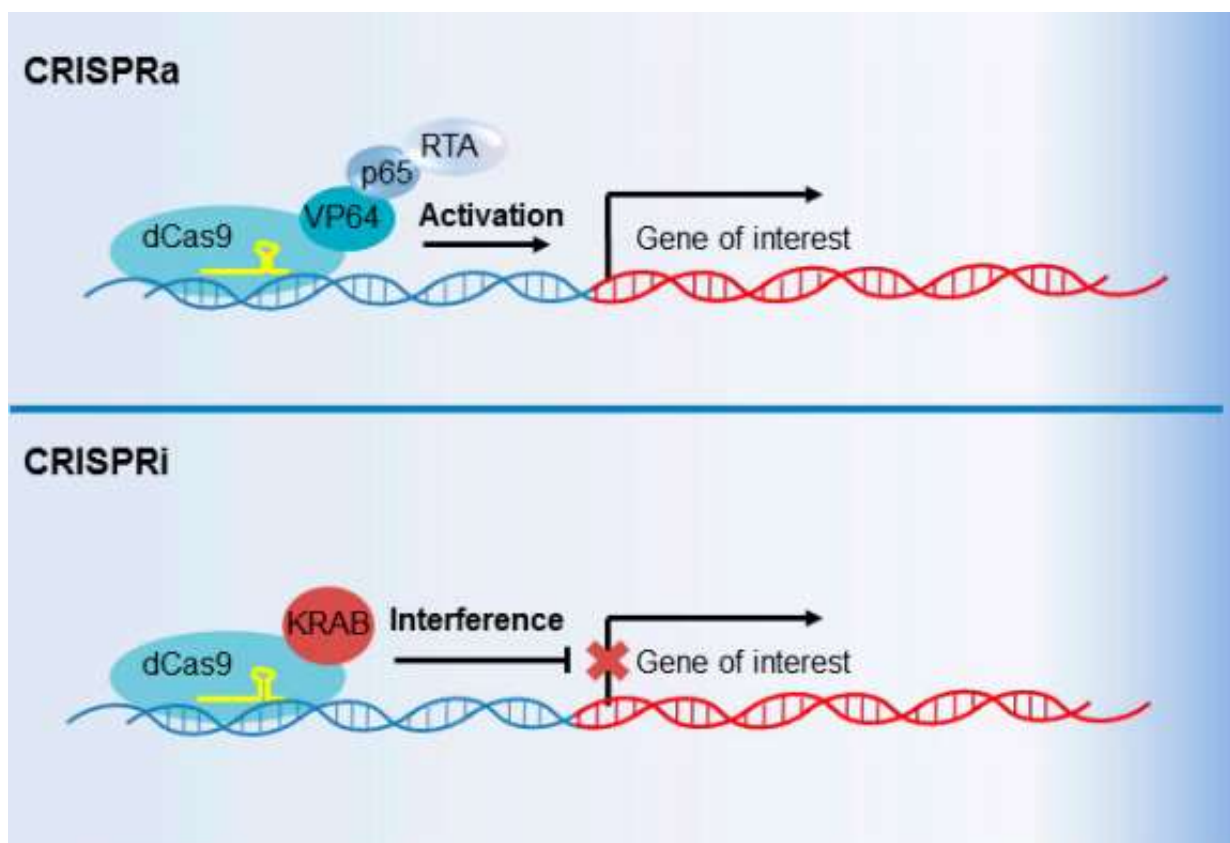
Figure 5: Overview of CRISPR activation (CRISPRa) and CRISPR interference (CRISPRi). For Cas9 nuclease-mediated knockout, double-strand break (DSB) formation is followed by non-homologous end-joining (NHEJ) DNA repair that can introduce an indel mutation and a coding frameshift. For dCas9-mediated transcriptional modulation, the SAM complex is necessary (Gebre, Nomburg, & Gewurz, 2018).

1.3.1 Genome-scale transcriptional activation screen by an engineered CRISPR-dCas9 complex

Recently, a screen combining the RNA-guided CRISPR-associated dCas9 nuclease with genome-scale gRNA libraries was applied to investigate resistance mechanism to BRAF inhibitor. The top significant candidates included genes previously shown to correlate with resistance and novel candidates were validated using individual sgRNAs. The results were also comparable with cDNA overexpression experiments (Konermann et al., 2015; Shalem et al., 2015). This finding demonstrated the potential of applying this approach as a powerful genetic perturbation technology to investigate resistant mechanism for inhibitors.

1.4 Aims

Our group has already demonstrated that CDK4/6 inhibition is a promising approach for treatment of bladder cancer in preclinical research (Sathe et al., 2016). However, the molecular determinants of treatment response and the development of biomarkers to enable patient stratification are still have to be clucidated.

In this work, we aimed to reveal molecular mechanisms that confer resistance to Palbociclib in order to

1. Identify predictive marker.
2. Identify suitable combination therapies in order to overcome resistance.

Experimental design:

Perform a CRISPR/dCas9 GOF screen on a bladder cancer cell line under treatment of Palbociclib.

ı CRISPR screen for resistance to Palbociclib in T24SAM cell line

ı Establishment of T24 cells expressing the SAM system.

ⅱ Amplification of sgRNA library which targeting genome-wide encoding refseq isoforms and validation of the library representation.

ⅲ Lentivirus package of amplified sgRNA library.

ⅳ Antibiotic selection for positive transfected T24SAM cells expressing the sgRNA library.

ⅴ Extraction of genomic DNA from treatment and control group.

ⅵ NGS analysis with DNA samples.

Ⅱ sgRNA enrichment analysis with MaGeck to reveal candidate sgRNAs induce resistance to Palbociclib.

Functional validation of the Screen candidates

Ⅲ Validation of significant candidate sgRNAs.

Ⅳ Bioinformatics' analysis with significant sgRNAs to reveal potential pathway which when activation may confer resistance to Palbociclib.

Clinical translation of the screen result: combination therapies and patient stratification

Ⅴ Identification of potential combination therapies.

Ⅵ Detection of anti-tumor effects with identified combination therapies in vitro and in 3-D model.

Ⅶ Analysis of molecular mechanisms of synergistic combination therapies.

Ⅷ Development of a model for the pre--stratification of patients for mono or combination therapy based on the screen results and TCGA dataset..

2 Materials

2.1 Multiple use equipment

Equipments and machines	Manufacturer
Autoclave Sytec DX-65	Systec GmbH, Linden, Germany
Biological safety cabinet Herasafe KS12	Thermo Scientific, Waltham, MA, USA
Analytical balance AT250	Mettler Toledo, Gießen, Germany
Analytical balance Sartorius 2254	Sartorius, Göttingen, Germany
Automatic film processor Curix CP1000	Agfa Healthcare, Mortsel, Belgium
BD FACSCalibur Flow Cytometry System	BD Biosciences, San Jose, CA, USA
BVC professional laboratory fluid aspirator	Vacuubrand Gmbh, Wertheim, Germany
Centrifuge ROTINA 35R	Hettich, Tuttlingen, Germany
Centrifuge 5810R	Eppendorf GmbH, Hamburg, Germany
Chemidoc™ XRS Imaging System	BioRad, Hercules, CA, USA
Cryogenic Freezing Container, 1 Deg C	Nalgene, Rochester, NY, USA
CO2 incubator HERA Cell240	Thermo Scientific, Waltham, MA, USA
Electrophoresis Power Supply EPS 601	Amersham Pharmacia Biotech., Uppsala, Schweden
Heating and drying oven Heraeus FunctionLine B6	Thermo Scientific, Waltham, MA, USA
Heating block thermostat BT100	Kleinfeld Labortechnik, Gehrden, Germany
Ice machine Manitowoc	Manitowoc Ice, Manitowoc, WI, USA
Intellimixer RM-2L	Elmi Ltd. Laboratory Equipment, Calabasas, CA, USA
Magnetic Stirrer	Heidolph Instruments GmbH, Schwabach, Germany
Microcentrifuge 5430R	Eppendorf GmbH, Hamburg, Germany
Mini-PROTEAN Tetra Cell gel system	BioRad, Hercules, CA, USA

Mini Trans-blot cell transfer system	BioRad, Hercules, CA, USA
Mini Protean System	BioRad, Hercules, CA, USA
Minishaker IKA® MS2	IKA Works Inc., Staufen, Germany
Multilabel plate reader VICTOR™ X3	Perkin Elmer, Waltham, MA, USA
Microplate reader Vmax Kinetic	Molecular Devices, Sunnyvale, CA, USA
Microscope camera AxioCam ERc 5s	Carl Zeiss, Oberkochen, Germany
Microscope AxioVert.135	Carl Zeiss, Oberkochen, Germany
Microscope AxioVert.A1	Carl Zeiss, Oberkochen, Germany
Micropipettes PIPETMAN P2, 10, 20, 200, 1000	BD Biosciences, San Jose, CA, USA
Neubauer chamber	LO Laboroptik, Lancing, England
Orbital shaker K15	Edmund Bühler GmbH, Hechingen, Germany
pH Meter 691	Metrohm, Filderstadt, Germany
Power supply PowerPac HC	BioRad, Hercules, CA, USA
PerfectBlue Gelsystem Mini M	PEQLAB Biotechnologie GmbH, Erlangen, Germany
Spectrophotometer Nanodrop 2000c	Thermo Scientific, Waltham, MA, USA
Thermal cycler C1000™ CFX96™	Bio-Rad, Hercules, CA, USA
Thermal cycler iCycler iQ ™ Real-time PCR detection system	BioRad, Hercules, CA, USA
Thermal cycler MJ Research PTC-200	BioRad, Hercules, CA, USA
Vortex-Genie® 2	Scientific Industries, Inc., Bohemia, NY, USA
Water bath W350	Memmert, Schwabach, Germany

Table 1: Multiple use equipment

2.2 Disposable equipment

Disposable equipments	Source
Amersham hybond-P PVDF-Membrane	GE-Healthcare, Buckinghamshire, England
Cell culture plates 96 well, 24 well, 12 well, 6 well, 10 cm	Coming Incoporated, Coming, NY, USA
Chromatography paper Whatman	GE Healthcare, Buckinghamshire, England
Conical bottom polystyrene tubes	Elkay, Hampshire, United Kingdom
Conical tubes 15ml, 50ml Falcon	Greiner GmbH, Frickenhausen, Germany
Cryogenic vials 1.8 ml Nunc	Sigma-Aldrich Chemie GmbH, Munich, Germany
Hard-Shell PCR Plates 96-well	BioRad, Hercules, CA, USA
Lens cleaning paper	The Tiffen company, Hauppauge, NY, USA
Microscope coverslips	Thermo Scientific Waltham, MA, USA
Microscope slides Superfrost plus	Thermo Scientific Waltham, MA, USA
Needles 27 Gauge	BD Biosciences, San Jose, CA, USA
PCR reaction tube 0.5 ml	Biozym Scientific, Oldendorf, Germany
PCR sealers Microseal 'B' Film	BioRad, Hercules, CA, USA
Pipette tips with and without filter	Sarstedt, Nuembrecht, Germany
Reaction tubes 0.5ml, 1.5ml, 2ml	Sarstedt, Nuembrecht, Germany
Serological pipettes	Greiner Bio-One International AG, Kremsmuenster, Austria
Silicone sheet, 0.5mm thick	Sahlberg GmbH&Co., KG, Munich, Germany
Sterile filter Nalgene 0.25µm, 0.45µm	Thermo Scientific, Waltham, MA, USA
Syringes 1ml Omnifix	B. Braun Melsungen AG, Melsungen, Germany
Ultracentrifugation tube Ultra-Clear 25x89 mm	Beckmann&Coulter GmbH, Krefeld, Germany
X-ray film CEA RP New	Agfa Healthcare, Mortsel, Belgium

Table 2: Disposable equipment

2.3 Chemicals, reagents and enzymes

Chemicals/reagents	Manufacturer
2-mercaptoethanol	Sigma-Aldrich Chemie GmbH, Munich, Germany
70 % Ethanol	BrüggemannAlcohol Heilbronn GmbH, Heilbornn, Germany
Acetic acid	Merck Chemicals GmbH, Hessen, Germany
Agarose	Thermo Scientific, Waltham, MA, USA
Ammonium persulfate (APS)	Sigma-Aldrich Chemie GmbH, Munich, Germany
Ampicillin	Sigma-Aldrich Chemie GmbH, Munich, Germany
Boric acid	Sigma-Aldrich Chemie GmbH, Munich, Germany
Bovine serum albumin (BSA)	Sigma-Aldrich, St. Louis, MO, USA
Bromophenol blue	Serva Electrophoresis GmbH, Heidelberg, Germany
Calcium chloride	Merck Chemicals GmbH, Hessen, Germany
Chlorophorm	Sigma-Aldrich Chemie GmbH, Munich, Germany
Citric acid	Sigma-Aldrich Chemie GmbH, Munich, Germany
Color Prestained Protein Standard, Broad Range (11–245 kDa)	New England Biolabs GmbH, Frankfurt, Germany
COMPLETE™, Mini protease inhibitor cocktail	Roche, Basel, Switzerland
Dimethyl sulfoxide (DMSO)	Sigma-Aldrich Chemie GmbH, Munich, Germany
Dithiothreitol (DTT)	Cell-Signaling, Cambridge, England

DNA ladder (100 bp and 1000 bp)	New England Biolabs GmbH, Frankfurt, Germany
DNA loading buffer (6 x)	Thermo Scientific, Waltham, MA, USA
Dulbecco's Modified Eagle's Medium (DMEM)	Biochrom, Merck Millipore, Berlin, Germany
E. coli, DH10B	PD Per Sonne Holm, Experimental Urology, Klinikum rechts der Isar, TUM
Ethanol absolute	Merck Chemicals GmbH, Hessen, Germany
Ethidiumbromide 10 mg/ml	Sigma-Aldrich Chemie GmbH, Munich, Germany
Ethylenediaminetetraacetic acid (EDTA), 0.5 M	AppliChem, Darmstadt, Germany
FastAP phosphatase	Thermo Scientific, Waltham, MA, USA
Fetal Bovine Serum (FBS)	Biochrom, Merck Millipore, Berlin, Germany
Formaldehyde (36.5 – 38 %)	Sigma-Aldrich Chemie GmbH, Munich, Germany
Fugene HD	Promega Corporation, Madison, WI, USA
Glycine	Sigma-Aldrich Chemie GmbH, Munich, Germany
GoTaq ® qPCR master mix	Promega, Madison, WI, USA
GoTaq ® Green PCR master mix	Promega, Madison, WI, USA
HEPES	Sigma-Aldrich Chemie GmbH, Munich, Germany
Hydrogen chloride (HCl)	Merck Chemicals GmbH, Hessen, Germany
Hydrogen peroxide	Merck Chemicals GmbH, Hessen, Germany
Isocitrate monohydrate	Sigma-Aldrich Chemie GmbH, Munich, Germany
Isopropanol	Sigma-Aldrich Chemie GmbH, Munich, Germany

L-Glutamin 200mM	Sigma-Aldrich Chemie GmbH, Munich, Germany
Lipofectamine RNAimax	Invitrogen, Carlsbad, CA, USA
Luminol	Sigma-Aldrich Chemie GmbH, Munich, Germany
Magnesium Chloride	Sigma-Aldrich Chemie GmbH, Munich, Germany
Methanol	Sigma-Aldrich Chemie GmbH, Munich, Germany
Non-essential amino acids (NEAA)	Biochrom, Merck Millipore, Berlin, Germany
Opti-MEM	Biochrom, Merck Millipore, Berlin, Germany
p-Coumaric acid	Sigma-Aldrich Chemie GmbH, Munich, Germany
Penicillin/Streptomycin	Sigma-Aldrich Chemie GmbH, Munich, Germany
Phosphate buffered saline (PBS)	Biochrom, Merck Millipore, Berlin, Germany
Phosphotase inhibitor Mix II	Serva Electrophoresis GmbH, Heidelberg, Germany
Phusion High-Fidelity PCR Master Mix	Thermo Scientific, Waltham, MA, USA
Polybrene	Sigma-Aldrich Chemie GmbH, Munich, Germany
Potassium chloride	Merck Chemicals GmbH, Hessen, Germany
Potassium hexacyanoferrate(II) trihydrate	Sigma-Aldrich Chemie GmbH, Munich, Germany
Potassium hexacyanoferrate(III)	Sigma-Aldrich Chemie GmbH, Munich, Germany
Puromycin	Sigma-Aldrich Chemie GmbH, Munich, Germany

Restriction enzyme buffers	New England Biolabs GmbH, Frankfurt, Germany
Restriction enzymes	New England Biolabs GmbH, Frankfurt, Germany
Roswell Park Memorial Institute medium (RPMI)	Biochrom, Merck Millipore, Berlin, Germany
Rotiphorese® gel 30	Carl Roth, Karlsruhe, Germany
Select agar	Sigma-Aldrich Chemie GmbH, Munich, Germany
Skimmed milk powder	Nestlé, Vevey, Switzerland
Sodium acetate	Merck, Darmstadt, Germany
Sodium azide	Sigma-Aldrich Chemie GmbH, Munich, Germany
Sodium chloride	Merck Chemicals GmbH, Hessen, Germany
Sodium dodecyl sulfate (SDS)	Sigma-Aldrich Chemie GmbH, Munich, Germany
Sodium orthovanadate	Sigma-Aldrich Chemie GmbH, Munich, Germany
Sodium phosphate dibasic	Merck Chemicals GmbH, Hessen, Germany
Sulforhodamin B (SRB)	Sigma-Aldrich Chemie GmbH, Munich, Germany
T4 DNA Ligase	Thermo Scientific, Waltham, MA, USA
Tetramethylethylenediamine (TEMED)	Carl Roth, Karlsruhe, Germany
Trichloroacetic acid	Sigma-Aldrich Chemie GmbH, Munich, Germany
Tris(hydroxymethyl)-aminomethan	Merck Chemicals GmbH, Hessen, Germany
Triton X100	Sigma-Aldrich Chemie GmbH, Munich, Germany
Trypan blue	Biochrom, Merck Millipore, Berlin, Germany

Trypsin/EDTA	Biochrom, Merck Millipore, Berlin, Germany
Tween-20	Serva Electrophoresis GmbH, Heidelberg, Germany

Table 3: Chemicals, reagents and enzymes

2.4 Commercial kits

Commercial kits or assays	Source
CellTiter-Blue® Cell Viability Assay	Promega, Madison, WI, USA
Click-iT™ EdU Alexa Fluor™ 488 Imaging Kit	Thermo Scientific, Waltham, MA, USA
High capacity cDNA reverse transcription kit	Thermo Scientific, Waltham, MA, USA
HiSpeed® Plasmid Midi Kit	Qiagen, Hilden, Germany
mirVANA miRNA isolation kit	Thermo Scientific, Waltham, MA, USA
Pierce™ BCA Protein Assay Kit	Thermo Scientific, Waltham, MA, USA
QIAprep® Spin Miniprep Kit	Qiagen, Hilden, Germany
QIAquick gel extraction kit	Qiagen, Hilden, Germany

Table 4: Commercial kits

2.5 Buffers and solutions

Buffer	Components
0.2 M Citric acid/sodium phosphate buffer	36.85 ml of 100 mM citric acid
	63.15 ml of 200 mM sodium phosphate dibasic
	pH=6
0.5 % (W/V) SRB staining solution	0.5 % SRB in 1 % acetic acid
1 % SDS Protein lysis buffer (REFERENCE)	1 % SDS
	10 mM Tris/HCl, pH=7.2
	1 mM sodium orthovanadate

	1 Complete Mini-Protease Inhibitor tablet and 100 ul of phosphatase inhibitor were added to 10 ml of lysis buffer before use
10 x SDS page running buffer (10 x TGS)	25 nM Tris 192 mM Glycine 0.1 % w/v SDS
10 x TBE	1 M Tris 1 M Boric acid 0.02 M EDTA
10 x TBS	0.5 M Tris-HCl, pH=7.6
10 x Transfer buffer	25 nM Tris 192 mM Glycine 20 % Methanol
100 % TCA	0.3 M TCA in 22.7 ml dH2O
2 x HBS	8 g sodium chloride 0.38 g potassium chloride 0.1 g sodium phosphate dibasic 5 g hepes 1 g glucose Add deioneizd water to 500ml, adjust pH to 7.05
4 x Protein loading buffer	0.25 M Tris-HCl, pH=6.8 8 % SDS 0.04 % Bromophenol blue 40 % Glycerine The above solution and 1 M DTT were mixed with a ratio of 5 to 1 before use

Chemiluminescence reagent	Chemiluminescence reagent part A and B were mixed with a ratio of 1 to 1 before use
Chemiluminescence reagent part A	0.1 M Tris-HCl, pH=8.5 2.5 mM Luminol 0.4 mM p-Coumaric acid
Chemiluminescence reagent part B	0.1 M Tris-HCl, pH=8.5 0.18 % hydrogen peroxide
Immunoblotting antibody dilution buffer	5 % BSA and 0.02 % sodium azide in TBS-T
Immunoblotting blocking solution	5 % skimmed milk powder in TBS-T
SA-BGal staining solution	2 ml of 0.2 M Citric acid/sodium phosphate buffer 0.5 ml of 100 mM Potassium hexacyanoferrate(II) 0.5 ml of 100 mM Potassium hexacyanoferrate(III) 300 ul of 5 M sodium chloride 20 ul of 1 M Magnesium Chloride 0.5 ml of fresh-made 20 mg/ml 6.18 ml of deionized water
Separating gel buffer	1.5 M Tris-HCl, pH=8.8
Stacking gel buffer	0.5 M Tris-HCl, pH=6.8
TBS-T	0.1 % Tween-20 in 1 x TBE

Table 5: Buffers and solutions

2.6 Antibodies

Antibodies	Dilution	Source
CDK2 (78B2)	1:1000	CST, Beverly, MA, USA

Akt (pan) (C67E7)	1:1000	CST, Beverly, MA, USA
Phospho-Akt (Thr308) (C31E5E)	1:1000	CST, Beverly, MA, USA
Phospho-p70 S6 Kinase (Thr389) (108D2)	1:1000	CST, Beverly, MA, USA
p70 S6 Kinase	1:1000	CST, Beverly, MA, USA
Phospho-p44/42 MAPK (Erk1/2) (Thr202/Tyr204) (20G11)	1:1000	CST, Beverly, MA, USA
p44/42 MAPK (Erk1/2)	1:1000	CST, Beverly, MA, USA
Phospho-Rb (Ser780)	1:1000	CST, Beverly, MA, USA
Rb, 554136	2 µg/ml	BD Bioscience, San Jose, CA, USA
GAPDH (14C10)	1:1000	CST, Beverly, MA, USA
Cyclin D1 (92G2)	1:1000	CST, Beverly, MA, USA
Phospho-CDK2 (Thr160)	1:1000	CST, Beverly, MA, USA
Anti-Cas9, clone 7A9 (Cat. #MAC133)	1:1000	EMD Millipore Corporation, Ontario, Canada
Peroxidase conjugated anti-mouse IgG, 715-036-150	1:10000	Dianova GmbH, Hamburg, Germany
Peroxidase conjugated anti-rabbit IgG, 711-036-152	1:10000	Dianova GmbH, Hamburg, Germany

Table 6: Antibodies

2.7 sgRNA sequences

Name	Forward sequence: 5' – 3'	Reverse sequence: 5' – 3'
HNF1B gRNA	CACCGGAGAGCCGGAGGGGCAGACC	AAACGGTCTGCCCCTCCGGCTCTCC
TGFB1I1 gRNA	CACCGCGCCTCCGCGGCAGGCCGGC	AAACGCCGGCCTGCCGCGGAGGCGC
RCAN3 gRNA	CACCGGGACAAGGCGGGGACCCGGG	AAACCCCGGGTCCCCGCCTTGTCCC

FAHD2B gRNA	CACCGCGGAGGGCGGGCCCAGTGCG	AAACCGCACTGGGCCCGCCCTCCGC
P4HA1 gRNA	CACCGGGGATGTAACGCGCCTGCGC	AAACGCGCAGGCGCGTTACATCCCC
MAP3K20 gRNA	CACCGCGGGGCGGATGGTGCCCCCC	AAACGGGGGGCACCATCCGCCCCGC
ZNF786 gRNA	CACCGCTGAGGGCGCCCGGGCCCCT	AAACAGGGGCCCGGGCGCCCTCAGC
UBA52 gRNA	CACCGCGCCCACCCGCTTCCGGTTG	AAACCAACCGGAAGCGGGTGGGCGC
Non-target control gRNA	CACCGACGGAGGCTAAGCGTCGCAA	AAACTTGCGACGCTTAGCCTCCGTC
KDR gRNA	CACCGGAGATCGCCGCCGGGTACCC	AAACGGGTACCCGGCGGCGATCTCC
FGFR3 gRNA	CACCGCGTGGCCGGGCGGGGGCGCC	AAACGGCGCCCCCGCCCGGCCACGC
AKT3 gRNA	CACCGCAGAAGAATCGCTTGAACCT	AAACAGGTTCAAGCGATTCTTCTGC
JAK2 gRNA	CACCGCTCAACGCCGCGGGCGACAC	AAACGTGTCGCCCGCGGCGTTGAGC
STAT3 gRNA	CACCGGGCTGTACCGCACACGCACT	AAACAGTGCGTGTGCGGTACAGCCC

Table 7: sgRNA sequences

2.8 Primer sequences

Name	Forward sequence: 5' – 3'	Reverse sequence: 5' – 3'
MS2-p65-HSF1	CCAGGCCTACAAGGTGACAT	GCCTTCACGATGAGTTCACA
gRNAs sequence	GCTTTATATATCTTGTGGAAAGGACGAAACACC	GCCAAGTTGATAACGGACTAGCCTT
HNF1B gene	ATGCTCAGTGAGGACCCTTG	GCAGCTGATCCTGACTGCTT
TGFB1I1 gene	CATGGAGGACCTGGATGCC	CCGCTGGAAGAGGAGAATGG
RCAN3 gene	GCCTCTCCAGCAGTGGGT	TCCCTCAGCATTATCCCCCA
FAHD2B gene	AAGCACATCAAGGCCACAGA	CAGCCACTGTTTCCCATTGC
P4HA1 gene	ACAGGAGACTTGGAGACGGT	TGGCTCATCTTTCCGTGCAA

MAP3K20 gene	TTCAACTCCTAACTGCGGCG	TACTTCCACAAAATCTGGCTCC
ZNF786 gene	CGGAGACGGTCGGGTTTG	AAAAGTCAGAGGTAGCCGAGG
UBA52 gene	CTTTTTCTTCAGCGAGGCGG	GCAGGGTGGACTCTTTCTGG
KDR gene	GAGGGGAACTGAAGACAGGC	GGCCAAGAGGCTTACCTAGC
FGFR3 gene	AGTGACGTCTGGTCCTTTGG	GGACGTCACGGTAAGGACAC
AKT3 gene	TTTTCTCTATTATTTGGGCTGAGTC	CCCCTCTTCTGAACCCAACC
JAK2 gene	CCGATCTGTGTAGCCGGTTT	GTAAGGCAGGCCATTCCCAT
STAT3 gene	GGAGAAACAGGATGGCCCAA	ATCCAAGGGGCCAGAAACTG

Table 8: Primer sequences

2.9 Plasmids

Plasmid	Source
Human CRISPR Activation Pooled Library (SAM v1)	Addgene, Cambridge, MA, USA

Table 9: Plasmids

2.10 Software for analysis

Name	Manufacture
CompuSyn	Combo Syn Inc., Parasmus, NJ, USA
FlowJo	FlowJo LLC, Ashland, OR, USA
GraphPad	GraphPad Software Inc., La Jolla, CA, USA
Mageck-VISPR	Dr. Xiaole Shirley Liu's lab, Harvard School of Public Health,MA,USA

Table 10: Software for analysis

2.11 Small molecule inhibitors

Small molecule inhibitors	Source
Roscovitine	Sigma-Aldrich Chemie GmbH, Munich, Germany
Palbociclib	Sigma-Aldrich Chemie GmbH, Munich, Germany
Everolimus	Selleckchem, Munich, Germany
Ruxolitinib	Selleckchem, Munich, Germany
Stattic	Selleckchem, Munich, Germany
SH-4-54	Selleckchem, Munich, Germany
Erdafitinib	Selleckchem, Munich, Germany
Axitinib	Selleckchem, Munich, Germany
CI-1040	Selleckchem, Munich, Germany
NVP-BEZ235	Selleckchem, Munich, Germany
MK-2206	Active Biochem, Bonn, Germany
PIK-90	Merck Chemicals GmbH, Darmstadt, Germany

Table 11: Small molecule inhibitors

3 Methods

3.1 Cell culture

3.1.1 Cell lines sub-culture

HEK293T, RT112 Luciferase cells (gifts from Dr. Per Sonne Holm, Department of Urology, TUM), RT112 from the Leibniz institute German collection of microorganisms and cell cultures (Braunschweig, Germany) and T24 cells (ATCC, Manassas, VA, USA) were maintained in DMEM or RPMI medium in 10% or 5% CO_2 respectively, supplemented with 10% FBS, 1% P&S and 1% NEAA at 37℃. Cells were passaged when reaching 70% confluency. All buffers and mediums for cell culture were pre-warmed to 37 ℃ before use. Cells were washed twice with PBS containing 5% 0.5 M EDTA after aspirating existing medium and incubating with trypsin at 37℃ until the cells rounded up and started to detach. Fresh medium was added immediately to neutralize the tryspin. Cells were harvested and centrifuged at 300 RCF for 5 minutes, resuspended and seeded into new 10 cm plates with a dilution of 1:10 to 1:2.

3.1.2 Cell counting

Cell suspension was diluted in equal volume of 0.5% trypan blue and cell number was counted in Neubauer chamber. Only unstained cells were counted as viable cells.

3.1.3 Cyropreservation of cell lines

Cells were harvested using PBS and trypsin as described above. Following centrifugation of cells, the pellet was re-suspended in 1 ml of freezing medium (10 % DMSO, 40% medium and 50 % FBS) and transferred into cryovials. They were transported using a freezing container and stored at −80℃ for 48-72 hours before transferring to liquid nitrogen. When thawing frozen cells for use, the cryovial was immersed in a water bath to ensure quick thawing of the freezing medium. To thaw frozen cells, the cryovials were incubated in 37 ℃ water bath for 1 minute. Cells were washed and then resuspended with 10 ml fresh medium before they were centrifuged and seeded back into a 10 cm plate.

3.2 Amplification of Human CRISPR Activation Pooled Library library (SAM v1) from Addgene

3.2.1 Electroporation of pooled Human CRISPR Activation Pooled library (SAM v1)

Human CRISPR 3-plasmid activation pooled library (SAM) was a gift from Feng Zhang (Addgene #61426) (Konermann et al., 2015). SAM library was supplied as 50ng/µLin UltraPure water. Endura electrocompetent cells (Lucigen Corporation, Middleton, WI, USA) were thawed on ice and mixed by gentle flicking and transferred to chilled micro centriguge tubes with 25ul for each. 2ul library DNA was added to each tube and mixed by gentle stirring but no pipetting (to avoid bubbles). Then the mix were transferred to the bottom of a chilled cuvette without any bubble. Then the electroporation was conducted with BioRad Genepulser II (Bio-Rad Laboratories GmbH, Munich, Germany) with 1.8 kV, 600 Ohm, 10 µF, 3.5 to 4.5 milliseconds time constant. 975ul pre-warmed recovery medium was added immediately and mixed gently twice with a pipette and transferred to a 17 100mm culture tube. Added an additional 1ml to wash the cuvette and transferred into the same culture tube. All 8 electroporations were done as same and shaked at 250rpm at 37℃ for 1 hour. In total all 16 ml were pooled and well mixed.

3.2.2 Calculation of transformation efficiency

20ul of the bacterial suspension above was taken and mixed with 1 ml recovery medium. 100ul of this mixture was plated onto a pre-warmed agarose plate (Ampicillin resistance). The number of colonies was calculated after incubation at 32℃ for 14 hours and multiplied by 8000. To maintain at least 100-fold representation of the library, a minimum $7*10^6$ colonies in total were required, so at least 875 colonies on the plate.

3.2.3 Plate the transformations

Each of 200ul of the 16 ml mixture above was spread onto in total 80 pre-warmed petri dishes (Ampicillin resistance) and dishes were incubated at 32℃ for 14 hours.

3.2.4 Colonies harvest and DNA extraction

1ml LB medium was added to each plate and colonies were scraped with a cell spreader or scraper and collected into falcon tubes. Bacterial pellets were weighted to determine the proper number of maxiprep columns to use (0.45g/Maxi-prep). DNA was prepared using Qiagen EndoFree Plasmid Maxi Kit (Qiagen, Hilden, Germany) following the manufacturer's protocol. A NanoDrop UV spectrophotometer was used to quantify the resulting plasmid DNA.

3.3 Next-generation sequencing of the amplified sgRNA library

Unique barcode nucleotides were added as NGS primers that amplify the sgRNA target region with Illumina adaptor sequences. For the verification of the amplified SAM gRNA library, 10 ng of input plasmid DNA was used. To minimize error in amplifying sgRNAs, a Phusion Flash High-Fidelity PCR master mix (Life Technologies) was used for PCR with 28 cycles as 98 °C for 90 s, 98 °C for 1 s, 60 °C for 5 s, 72 °C for 15 s, followed by final extension of 72 °C for 1 minute. PCR products were pooled and purified by using the QIAquick PCR Purification Kit according to the manufacturer's directions.

The purified PCR products were quantified and run on a 2% (wt/vol) agarose gel. Interested product was extracted using Monarch DNA Gel extraction kit (NEB GmbH, Frankfurt, Germany) according to manufacturer's instructions. Amplicons were sequenced on an Illumina HiSeq platform by GATC Biotech (Konstanz, Germany) using coverage of 15 million reads per condition with 125bp PE (paired-end) sequencing, NGS libraries were prepared from amplicons by GATC Biotech (Konstanz, Germany) and 125 bp paired end sequencing was carried out on an Illumina HiSeq 4000 with 15 million reads.

3.4 Production of lentivirus containing sgRNA library and titer

3.4.1 Lentivirus package

Lentivirus was produced as described (Nawroth et al., 2007). 2 million 293T cells were seeded on 10 cm plates and transfected with 20 ug of gRNA plasmid, 15 ug of psPASX2 and 6 ug pMD2.G using 2.5 M CaCl2 and 2x HBS, in total 50 plates. Medium was changed 6 hours after transfection and virus supernatant was collected and pooled together after 48 hours. The virus supernatant was centrifuged at 1000rpm and flited with 0.45um filter, then stored at 4 °C until titration is completed in parallel.

3.4.2 Functional titration of lentivirus

Different volumes of viral supernatant were applied to T24 cells in a 6 well format and treated with selection antibiotics for 72 hours. Cell viability was determined by SRB assay, and the multiplicity of infection (MOI) for the virus was calculated as described (Sanjana, Shalem, & Zhang, 2014).In brief, we used functional titration: percent of cells that can survive antibiotic selection, which correlates with number of functional infectious viral particles. A volume which correlated with a MOI 0.1(with certain volume of viral supernatant, 10% cells survived under Zeocin selection) was chosen for further experiments, which should guaranty more than 90% positively selected cells have only been infected by one functional partial of lentivirus.

3.5 Generation of T24 SAM cells with lentivirus transduction

T24 cells were transduced with lentivirus containing dCas9-VP64 and MS2-p65-HSF1 respectively (Konermann et al., 2015). Antibiotics (blasticidin, hygromycin B from Life Technologies) for selection pressure were applied to the cells 24 hours after transduction and selection pressure was continued for 8 days. Monoclonal colonies were isolated and expression of dCas9-VP64 and MS2-p65-HSF1 were measured with WB and PCR.

3.6 Screen of resistance to Palbociclib

3.6.1 Expansion of T24 SAM cells and transduction with the lentiviral sgRNA library

T24 SAM cells were expanded to at least 350 million and transduced with Lentivirus from 3.4.1 at 0.1 MOI. Then 300ug/ml zeocin was applied as selection pressure for positively infection. Fresh medium with antibiotic was changed every two days, in total selection period was 8 days.

3.6.2 Palbociclib resistance screen

The surviving T24 SAM cells were divided into control (non-treatment) and treatment group. Palbociclib at 1000nm was applied to the treatment group with daily fresh medium containing Palbociclib change. The treatment lasted for 7 days in total. In total 3 independent biological replicates for control and treatment condition were performed.

3.6.3 Genomic DNA (gDNA) extraction

All cells were trypsinized carefully and centrifuged at 1000 rpm. 6 ml of NK lysis buffer (50 mM Tris HCl pH 8, 50 mM EDTA, 1% SDS) were added to each cell pellet with 30 ul of 20mg/ml Proteinase K and incubated at 55 ℃ overnight. 30 ul of 10mg/ml RNAse A was added on the next day and the tubes were inverted around 25 times and incubated at 37 ℃ for 30 minutes and cooled down on ice. 2 ml of pre-chilled 7.5 M Ammonium acetate was added to precipitate proteins. Then all tubes were vortexed at high speed and spin down at 6000 g for 20 min, and supernatant was transferred into a new tube. After adding 6 ml of 100% isopropanol, 50 times inverting followed. DNA pellets were visible after 20 min. spinning at 6000g. The supernatant was discarded and pellets were placed under a hood for air dry. Each pellet was resuspended with 500ul TE buffer at 65℃ for 1 hour. Concentration and quality of DNA were measured using a Nanodrop 2000c.

3.6.4 Amplification and purification of gDNA for Next-Generation-Sequencing (NGS)

In order to maintain representation, PCR was carried out on genomic DNA equivalent to 500 cells per guide, corresponding to a total of 231ug from 35 million cells (assuming 6.6 pg in a single diploid cell). PCR was conducted using Phusion Flash High-Fidelity PCR master mix (Life Technologies) for 28 cycles as 98 ℃ for 90 s, 98 ℃ for 1 s, 60 ℃ for 5 s, 72 ℃ for 15 s, followed by final extension of 72 ℃ for 1 minute. To enable multiplexing during NGS, an 8 bp unique barcode was added at the beginning of the forward primer as TCGCCTTG, ATAGCGTC, GAAGAAGT, ATTCTAGG or CGTTACCA. Then all PCR products were pooled together in a 50 ml Falcon tube with 1/10 volume of 3M Sodium Acetate. 2.5 volume of 100% ethanol was well mixed in addition and incubated at room temperature for 5 minutes. Supernatant was removed after centrifugation at 20000g for 15 minutes. The pellet was washed carefully twice with 70% ethanol and re-suspend in EB buffer. Gel electrophoresis was conducted on a 2% agarose gel. The band of interest was extracted using Monarch DNA Gel extraction kit (NEB GmbH, Frankfurt, Germany) according to manufacturer's instructions.

3.6.5 Next-generation sequencing of the amplified sgRNA library

Amplicons were sequenced on an Illumina HiSeq platform by GATC Biotech (Konstanz, Germany) using coverage of 15 million reads per condition with 125bp PE (paired-end) sequencing, NGS libraries were prepared from amplicons by GATC Biotech (Konstanz, Germany) and 125 bp paired end sequencing was carried out on an Illumina HiSeq 4000 with 15 million reads per condition.

3.6.6 Analysis of NGS data

FastQC was used for quality control of NGS data at the sequence level (Andrews, 2010). NGS reads were demultiplexed according to the 8 bp barcode in the forward primer using cutadapt (MARTIN, 2011). Adapter and primer sequences were trimmed using cutadapt to yield 20 bp gRNA sequences, with no mismatches permitted for both steps. Screen hit identification, quality control and visualization were performed using MAGeCK-VISPR (version 0.5.7)(Li et al., 2015; Li et al., 2014). 'count' and 'test' commands from MAGeCK were used with default parameters and zero count removal. A list of human housekeeping genes were applied as biologically negative control (Eisenberg & Levanon, 2013). MAGeCK results were then used as input for VISPR.

3.6.7 Bioinformatics analysis with screen results

Pathway analysis of candidate genes was performed using DAVID V 6.8, Reactome Version 65 (Fabregat et al., 2018; Huang da, Sherman, & Lempicki, 2009).

3.6.8 Validation of candidate sgRNAs

sgRNAs and validated non-target control sgRNA *(Bao et al., 2016) were cloned* into lenti-sgRNA(MS2)-zeo-backbone (addgene #61427) as described (Power & Izawa, 2016) and verified by Sanger sequencing. T24 SAM cells were transduced with lentivirus at MOI 0.05 and selected for zeocin resistance (300ug/ml). SgRNA expression and mRNA expression fold change were detected with qPCR as described in resulting polyclones (sgRNA sequences and primers are listed in Supplementary Table S2) (Sathe et al., 2016).

3.7 Treatment of cells with small molecule inhibitors

Inhibitors were dissolved in recommended vehicle and stored in 4 or -20 degree. Inhibitors for treatment were made fresh in pre-warmed medium. For inhibitors dissolved in DMSO, highest DMSO concentration was used as a control, so as for other stock.

3.8 Functional assays in vitro

3.8.1 Determination of cell viability and proliferation

Cell viability was determined using the Cell-Titer blue cell viability assay. The reagent was added into cell culture wells in a 1:10 ratio to the volume of culture medium, after 4-6 hours' incubation in cell culture incubator (avoiding light), the fluorescent was measured using 560nm and 580nm excitation and emission wavelengths respectively according to the manufacturer's protocol. Cell proliferation was detected with SRB assay. 10% TCA was used for cell fixation, after staining with 0.04% (wt/vol) SRB solution, unbound dye was washed away with 1% (vol/vol) acetic acid. Proper volume of 10 mM Tris base solution (pH 10.5) was applied on wells to solubilize the protein-bound dye. Then the absorbance was measured at 510 nm in a microplate reader. All experiments were performed in triplicates and repeated for at least 3 times.

3.8.2 Cell cycle analysis by flow cytometry

Cells were harvested and fixed in 75% cold ethanol overnight then washed with 1% BSA/PBS and stained using 4 ugs/mL 7-AAD according to the manufacturer's instructions. Flow cytometry was performed using FACSCanto II flow cytometer and analyzed with FlowJo v.7.6.4 software.

3.8.3 Clonogenic assay of cells *in vitro*

Cells were seeded in 6-well plates at a density of 30 cells per well and treated for 7 days with Palbociclib 1000nM. Medium containing inhibitor was replaced every second day. Colonies were fixed and stained (6% v/v glutaraldehyde and 0.5% w/v crystal violet) as described (Franken, Rodermond, Stap, Haveman, & van Bree, 2006) and microscopically visualized. More than 50 cells were regarded as a colony.

3.8.4 Combination Index

The dose-inhibitory fraction relationships for the combination therapy were assessed with the Chou–Talalay combination index (CI) analysis (Chou, 2006). We introduced redefined CI of additive effect as 0.9-1.1 while CI<0.9 as synergistic and CI>1.1 as antagonistic. The analysis was performed with ComboSyn.

3.9 3-Dimentional xenograft in vivo
The 3-Dimentional xenograft CAM assay was performed as described previously

(Skowron et al., 2017). In brief, 2 million RT112 Luc cells were seeded on ED (Embryo Day) 9 and topically treated with respective inhibitors on ED 11 – 14. Luminescence intensity was measured on ED 15 with HAMAMATSU Digital Camera C9016 (Hamamatsu Photonics K.K.) after adding D-Luciferin potassium salt (Sigma) and quantified with Simple PCI (Imaging Systems, Compix Inc. Cranberry Township, PA, USA).

3.10 Immunoblot

3.10.1 Preparation of cell lysates

All procedures were performed on ice. Cells were washed twice with pre-cold PBS. 500 ul or 100 ul of 1% SDS/RIPA lysis buffer was added to 10 cm or 6 well plates, respectively. Cell lysates were transferred to microcentrifuge tubes. 27-gauge needles and syringes were used for shearing DNA until viscosity was invisible if 1% SDS lysis buffer was applied. The samples were centrifuged at 30000 RCF for 30 minutes at 4 ℃.

The supernatants were used for further experiments or stored at -80 ℃.

3.10.2 Protein quantification and sample preparation

BCA protein assay was used to measure protein concentration of lysates according to manufacturer's protocol in 96-well plates. Briefly, 12.5 ul of protein samples or a series of protein standards were mixed with 112.5 ul of working reagent and incubated for 30 minutes at 37 ℃. Absorbance at 560nM was detected and the according protein concentration was calculated based on protein standards. All samples were diluted to equal protein concentration with lysis buffer and then mixed with 4x protein loading buffer containing 10% DTT. Samples were heated at 100 ℃ for 5 minutes for denaturation and stored at -20 ℃ for further experiments.

3.10.3 Sodium dodecyl sulfate polyacrylamide gel electrophoresis (SDS-PAGE)

Separating and stacking gel solutions were prepared as described in Table12 and 13. After complete polymerization (room temperature for 1 hour), 10 ul of molecular weight markers or 40 ul of protein samples were loaded into the wells of SDS-PAGE gel. Electrophoresis was performed at 90 V until samples run into separating gels and then continued at 150 V until the loading front moved to the bottom of gels.

Table 12: Recipe for separation gel

Ingredient	8 %	10 %	12 %
H2O [ml]	4.78	4.12	3.45
1.5M Tris pH 8.8[ml]	2.5	2.5	2.5
30% acrylamide/Bis-acrylamide solution [ml]	2.67	3.33	4
10% APS [µl]	50	50	50
TEMED [µl]	10	10	10
Total [ml]	10	10	10

Table 13: Recipe for stacking gel

Ingredient	
H2O [ml]	3.07
0.5M Tris pH 8.8 [ml]	1.25
30% acrylamide/Bis-acrylamide solution [ml]	0.65
10% APS [µl]	25
TEMED [µl]	5
Total [ml]	5

3.10.4 Transferring the protein to the membranes and blocking

The PVDF membranes were incubated in methanol for 5 minutes then washed extensively in the transfer buffer. The gels and membranes were assembled into transfer sandwiches. Then they were inserted into cassettes and placed into transfer tanks, with the membranes on the cathode and the gels on the anode. Transfer was performed at 4 ℃ for 2 hours at 100 V.

3.10.5 Immunodetection

The membranes were blocked with blocking buffer for 1 hour at room temperature, followed by an incubation with primary antibody solution overnight at 4 ℃. Membranes were washed with TBST buffer 5 times and then incubated with secondary antibody solution for 1 hour at room temperature. The membranes were washed with TBST buffer 5 times and incubated with Chemiluminescence reagent for 2 minutes. Chemiluminescent signals were captured using autoradiography films.

3.11 Real-time reverse transcription polymerase chain reaction (RT-qPCR)

3.11.1 RNA extraction

Extraction of total RNA from adherent cells in 6-well plates was performed using the mirVANA miRNA isolation kit according to the manufacturer's protocol. Then the extracted RNA was dissolved in Rnase-free water, RNA concentration and quality was detected using Nanodrop 2000c. The ratios of absorbance A260/A280 was between 1.8 and 2.0 were accepted for further applications. The purified RNA was stored at - 80 ℃ for next application.

3.11.2 cDNA synthesis

For each sample, 2 ug of total RNA from the above extraction was set as template for reverse transcription in a 20 ul system using High capacity cDNA reverse transcription kit (Thermo Scientific, USA) according to manufacturer's protocol.

3.11.3 Quantitative polymerase chain reaction (qPCR)

The reaction for qPCR was prepared in a 10 ul system consist of GoTaq qPCR Master mix with 50 ng of cDNA, 0.5 uM of forward and reverse primers. Each PCR reaction was run in triplicate in a CFX96 Real-Time PCR detection system. The cycling condition was set as follows: 94 ℃ for 2 minutes, 94 ℃ for 15 seconds, 60 ℃ for 30 seconds and 72 ℃ for 1 minute for 45 cycles. For quality control of the reaction, the melting curve from each reaction was examined first for the number of peaks. Then the amplified DNA products were loaded into agarose gel for electrophoresis to ensure the correct size of products and no formation of primer-dimer.

3.11.4 Relative quantification of gene transcription

Housekeeper gene GAPDH was used to normalize the transcription of target genes. The $\Delta\Delta$CT method was used for relative quantification of gene transcription as follows (Livak & Schmittgen, 2001):

ΔCT=CT (gene of target) – CT (GAPDH)

$\Delta\Delta$CT= ΔCT (treated sample) –ΔCT (control)

Relative gene expression = $2^{-\Delta\Delta CT}$

3.12 Graphical depiction and statistical comparison

Statistical analyses were performed using GraphPad Prism (version 6.0) software (GraphPad PrismSoftware, Inc). Data were analyzed for statistical significance using unpaired t-test/one-way ANOVA. For all experiments, $p < 0.05$ was considered statistically significant. Unless stated otherwise, all data were obtained from at least three independent experiments.

4 Results

4.1 The CDK4/6 inhibitor Palbociclib exhibited cell cycle arrest effect in RB positive bladder cancer cell lines accompanied with acquired resistance

We analyzed cell cycle distribution of T24 and RT112 cells under treatment of Palbociclib for 24 and 72 hours and observed that the cell cycle was arrested in G0/G1 phase at 24 hours. When treatment lasted for 72 hours, a partial recovery was detectable. This indicated that at later stages in the response to Palbociclib compensatory mechanisms partially reactivated cell cycle progression and resistance to CDK4/6 inhibition was established (Figure 6).
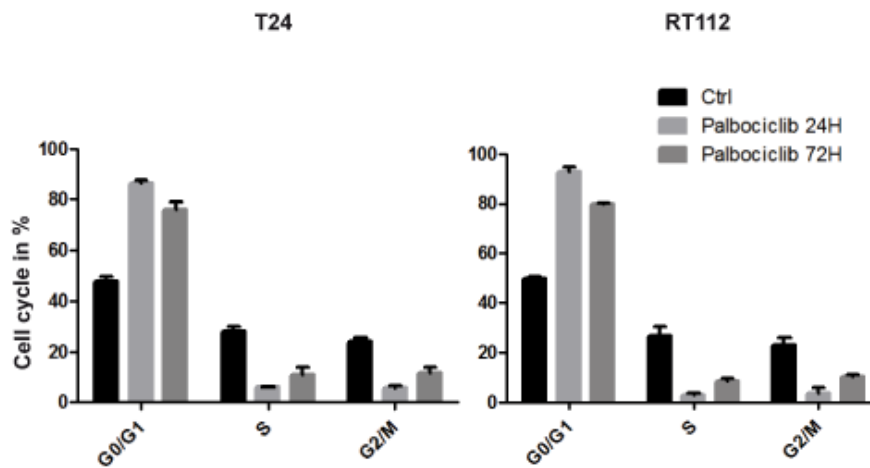
Figure 6: Cell cycle distribution under 1000nM Pabociclib treatment for 24H and 72H in T24 and RT112. Cell cycle distribution was analysed with FACS after 24H and 72H treatment in T24 and RT112 cell lines.

4.2 Genome-scale CRISPR/dCas9 transcriptional activation screen identified determinants of resistance to CDK4/6 inhibition

We utilized a forward genetics approach to determine resistance mechanisms to CDK4/6 inhibition. This was conducted by application of a genome-scale transcriptional activation screen using a CRISPR-dCas9 based system including a synergistic activation mediator (SAM) and a pool of 70290 sgRNAs (Konermann et al., 2015) as described schematically in Figure 7.
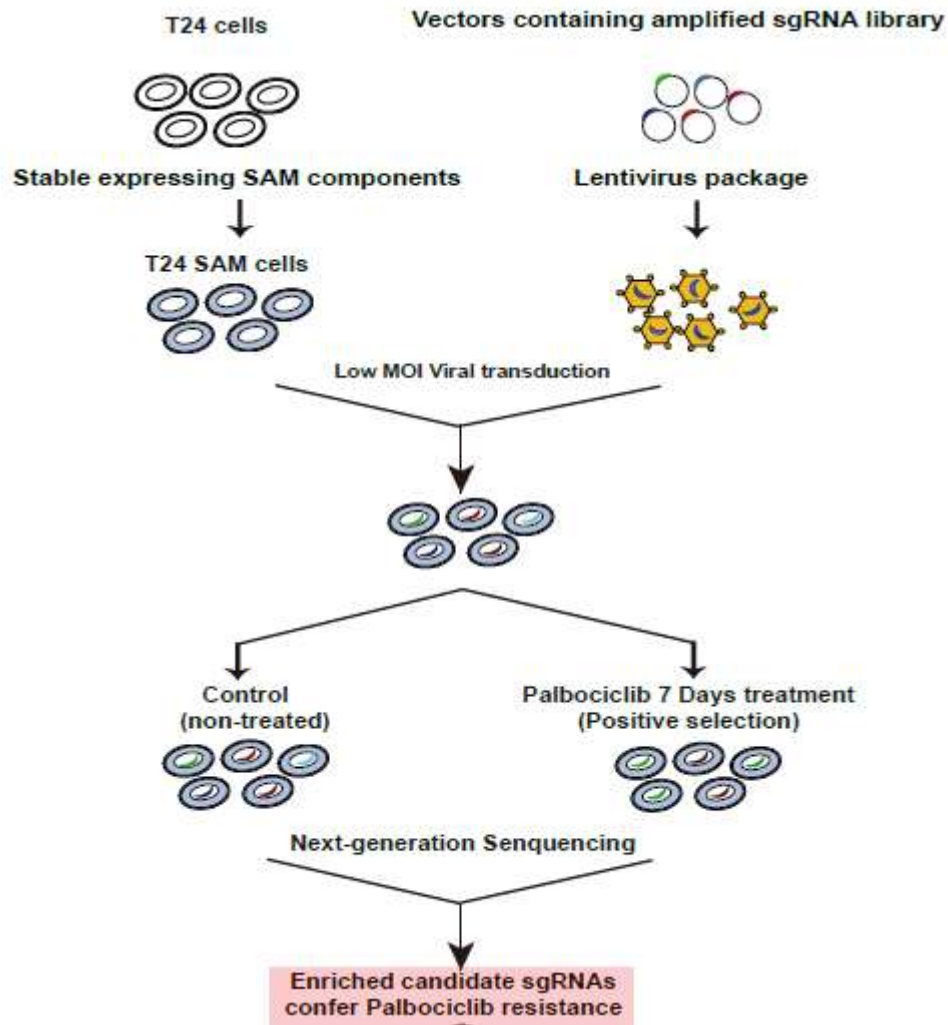
Figure 7: Schematic of CRISPR functional screen to resistance to Palbociclib on T24 SAM cells. Schematic of functional screening for candidate genes that confer resistance to CDK4/6 inhibition and translational workflow.

4.2.1 Expression of the SAM system in T24 cells by transfection

We first established multiple monoclones generated from T24 cells with lentivirus transduction (Methods 3.5) to express the synergistic activation mediator (SAM) components, dCas9-VP64 and MS2-p65-HSF1. Expression of the dCas9 protein was confirmed in multiple monoclones except in #7 by Western blot. The MS2-p65-HSF1 transcript was also confirmed in all clones by PCR (Figure 8). Clone #2 was used in the following gain of function screen[1].

---

[1] This part work was done together with Dr. Anuja Sathe.
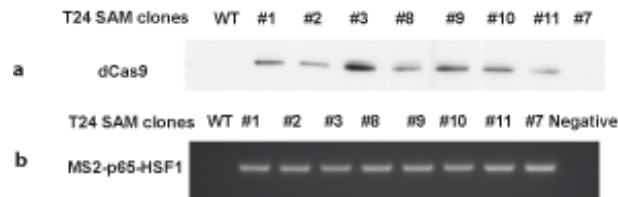
Figure 8: Characterization of T24 SAM clones. a expression of dCas9 detected by
WB. **b** MS2-P65-HSF1 activation helper detected by PCR.

4.2.2 Palbociclib exhibited anti-tumor effect in T24 and RT112 wild type cell lines and modified cell lines

Since the genetic modification and selection potentially can change characteristics of
a cell line, we tested the dose response to Palbociclib with T24 SAM cell line we
generated and also RT112luc cells that were derived from the RT112 cell line by a
stable transfection with a luciferase gene and used in this project. Both modified cell
lines, T24SAM and RT112luc responded to Palbociclib in a similar kinetic as wild
type cell lines, indicating the lentiviral transduction and followed selection processes
did not change their key response we needed for this research (Figure 9).
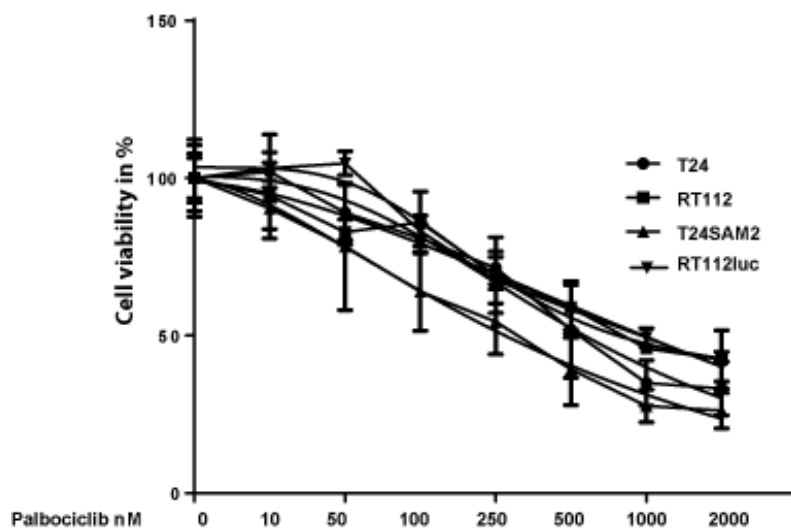
Figure 9: Dose response to Palbociclib with all cell lines used in this manuscript.
Response to all cell lines used to Palbociclib was evaluated with CTB assay.

4.2.3 T24 SAM cells expressing sgRNA library were screened for resistance to Palbociclib

After synthesis of virus in 293T cells, the cellular supernatant was tested for the viral titer. As shown in Figure 10, the virus was highly effective. 5 ul of virus supernatant infected 10% of cells based on functional titer result, which equals to MOI 0.1. Wit this MOI T24SAM cells were infected. Positively transduced T24 SAM cells were used as control or were treated with Palbociclib for 7 days. Genomic DNA was isolated and analyzed using next-generation sequencing. This screen was repeated in 3 independent replicates[2].
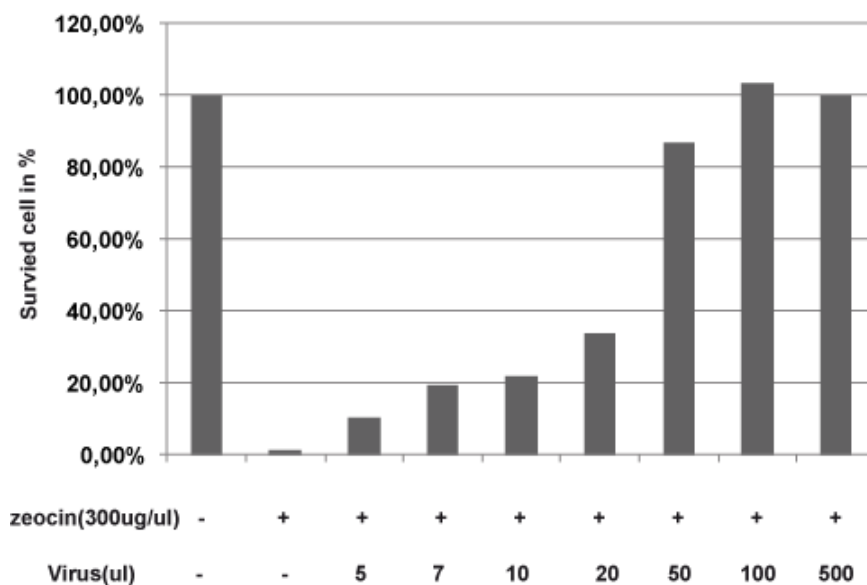
Figure 10: Functional titer with 300ug/ml Zeocin in T24SAM to determine MOI. Killing capacity of Zeocin 300ug/ml in T24 SAM cells with different MOI of lentivirus with SRB assay.

4.2.4 Quality control and analysis of NGS data

Each 3 replicates from control and treatment were grouped together with the SAM library and displayed similar sequence quality scores from 30-40 (error probability 0.001-0.0001), approximate mapped reads, read counts and Gini index (< 0.1) without skews (Figure 11 a,b,c,e). Comparison across the independent replicates revealed between 0.06-0.5% zero counts. In detail, 76 of 70290 sgRNAs were lost by amplification of the sgRNA library. Since each gene is targeted by 3 independent sgRNAs in the library, still 100% of the RefSeq coding isoforms were covered. Then in

---

[2] This work was done by Dr. Anuja Sathe

lentivirus package and transduction and Zeocin selection processes, we lost additional 72, 49 and 253 sgRNAs across the 3 control bio-replicates and 82, 122 and 355 in 3 bio-replicates of treatment group indicating that experimental conditions were adequate to maintain the sgRNA library representation (Figure 11f).

We used MaGeck to compare the differential expression of individual sgRNAs with the treatment and control replicates with both positive and negative selection approaches. We identified 1024 candidate sgRNAs that were significantly positive enriched with an FDR value < 0.1 in the treated cells which may confer resistance to Palbociclib (Figure 12, Figure 13b, Appendix Table 14).   We also noticed that some sgRNAs were negatively enriched which may mean activation of these targets may confer better response to Palbociclib (Figure 12). 3 sgRNAs were totally gone in more than one replicates of treatment which may indicate activation of this target may confer absolute response to Palbociclib, including NM_001173_16809, NM_001289984_27874 and NM_004499_35303 (Figure 12). These negative selection may be future direction to investigate response mechanism. Comparison of the read counts from control replicates and sgRNA library demonstrated a Pearson correlation coefficient value of 0.67-0.84 and between control and treatment replicates the value was 0.51-0.93 (Figure 13a). Three biological treatment replicates demonstrated a Pearson correlation coefficient value of 0.48-0.59 which was directly comparable to the original publication for this library (Konermann et al., 2015; Li et al., 2015).
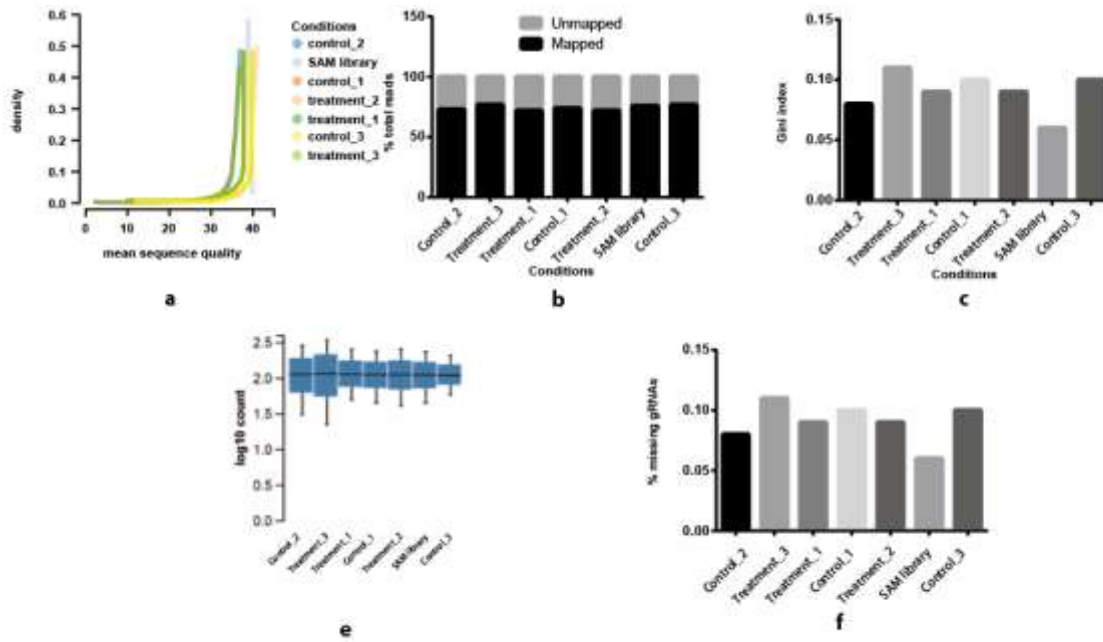
Figure 11: Quality control of NGS data using MaGeck-VISPR. "SAM library" indicates the amplified SAM library while 1, 2, 3 indicate independent bio-replicates of non-treated control and treatment with Palbociclib 1000nM. **a** sequence quality, **b** percentage of mapped reads, **c** Gini index, **e** count distribution, **f** percentage of missing gRNAs
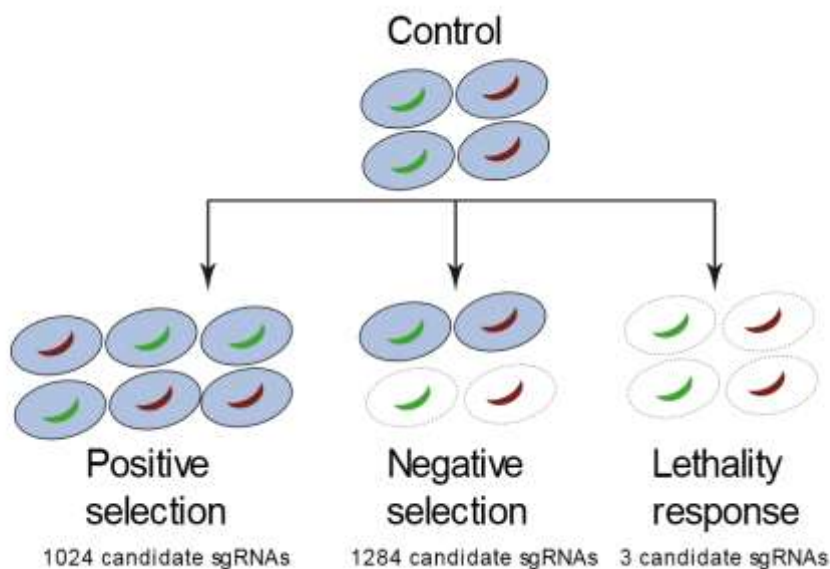
Figure 12: Analysis of significant sgRNAs. For positive selection, FDR cutoff value < 0.1, for negative selection, LFC cutoff value < -1. For lethality response, zero count was detected in more than one treatment replicate.
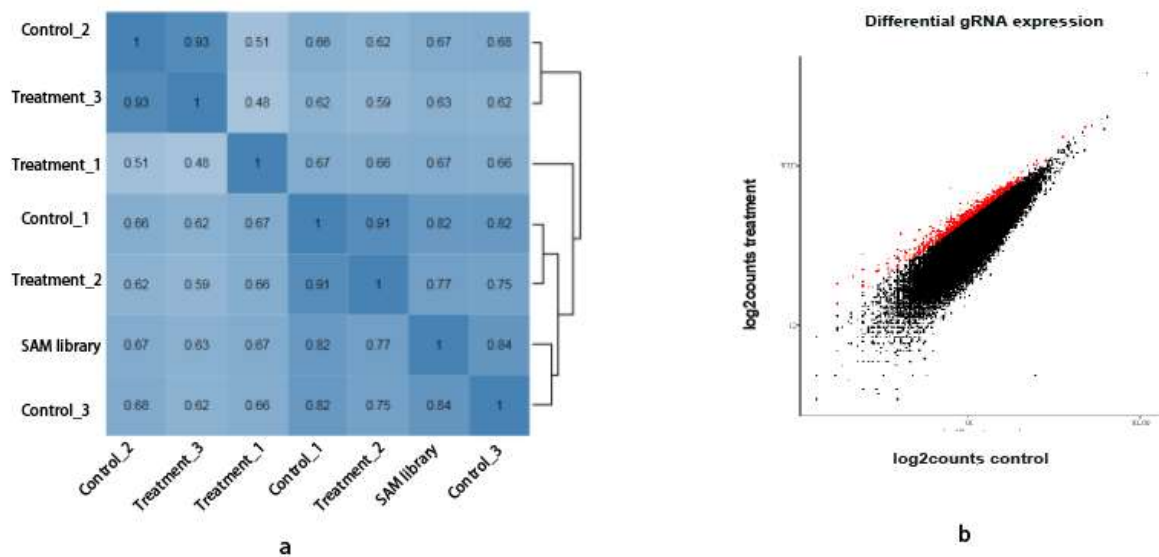
Figure 13: Analysis of positively enriched significant sgRNAs. Clustering and correlation. "SAM library" indicates analysis of the amplified SAM library while 1, 2, 3 indicate independent bio-replicates. **c** Individual gRNA counts were plotted for control and Palbociclib treatment conditions. Red dots indicate counts that are significantly enriched in Palbociclib treatment according to MAGeCK analysis, after applying cutoffs of p < 0. 1 (FDR corrected).

4.2.5 Validation of 8 significant sgRNA candidates confirm significance of the screen results obtained

Since such a genome-wide screening approach is prone to false negative or positive results, we performed biological validation on candidate sgRNAs. 8 sgRNAs which ranged in ranking within the first five hundred sgRNA candidates were randomly chosen, cloned into T24 SAM cells and examined for their effect on palbociclib treatment. These sgRNAs target proteins in the PAK pathway, TGF-β pathway, GPCR pathway, collagen chain trimerization, RNA Polymerase II Transcription Initiation and Promoter Clearance and Wnt pathway. Expression of all 8 sgRNAs transcripts (Figure 14a) and a 1.3 to 13-fold increase in the mRNA transcription level of the target genes as compared to non-target control sgRNA transduced cells (referred as NTC) was achieved (Figure 14b). All 8 sgRNAs induced increased proceeding into S-Phase under Palbociclib treatment (30-350%) as compared to NTC cells (Figure 14c). Significant increase in cell viability from 41% to 141% was noted after treatment after 72 hours in cells transduced with target sgRNAs compared to NTC (Figure 14d). This indicates that the acquired resistance induced by a single sgRNA confered partial

resistance to treatment. We also examined the effect of sgRNAs on survival and proliferation under long-term Palbociclib treatment using clonogenic assays conducted over 7 days. All sgRNAs induced up to 6-fold increased proliferation compared to NTC (Figure 14e,f).
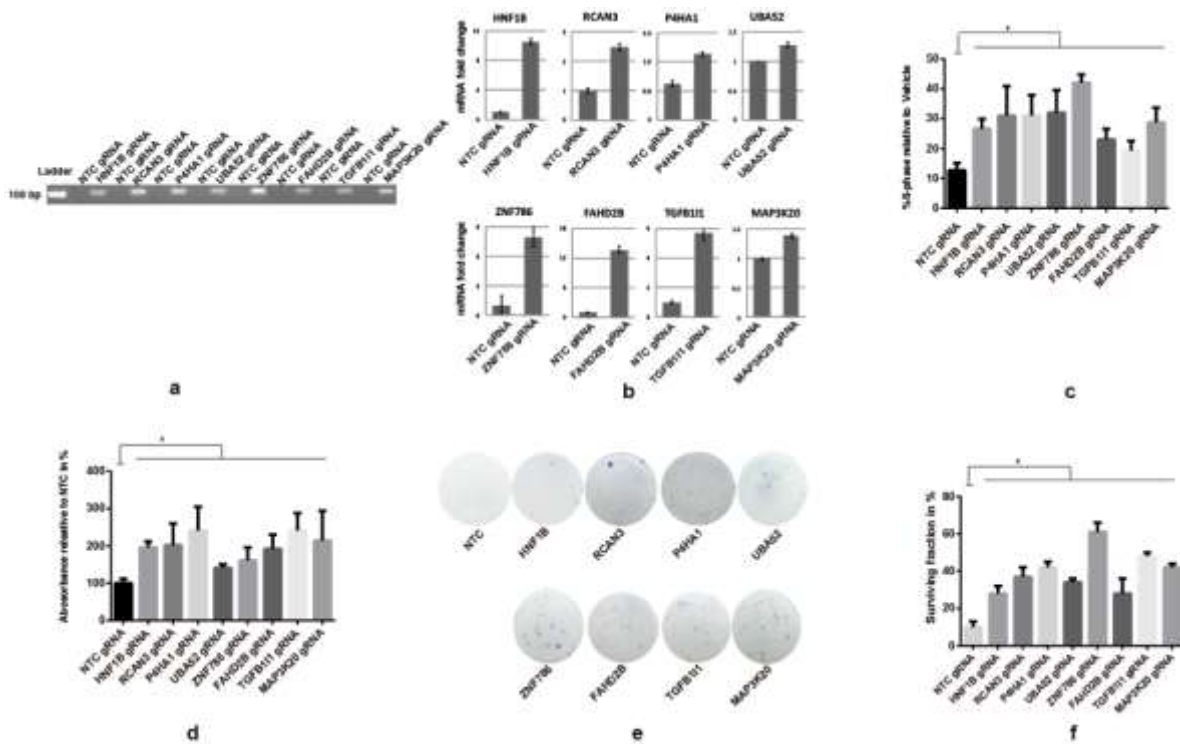
Figure 14: Validation for 8 significant candidate sgRNAs. a expression of selected sgRNA transcript sequences in engineered T24 SAM cells were analyzed by PCR. b transcriptional activation of the 8 candidate genes detected by qPCR. c In T24 SAM cells transduced with 8 significant sgRNAs, S-phase reduction was partially reversed under Palbociclib (1000nM) treatment 24H compared to non-treated control (*, P < 0.05; unpaired t-test compared to cells transduced with NTC gRNA). d SRB cell proliferation assay after 4 days of Palbociclib (1000nM) treatment (*, P < 0.05; unpaired t-test compared to cells transduced with NTC gRNA). e,f 10-day clonogenic assay under Palbociclib (1000nM) treatment, more than 50 cells were counted as a colony, surviving fraction = colony number/seeded cell number in % (*, P < 0.05; unpaired t-test compared to cells transduced with NTC gRNA). Data represent mean ± SD of 3 replicates.

4.2.6 Multiple pathways which may confer resistance to CDK4/6 inhibition were identified by bioinformatic analysis of NGS data

For analyzing the biological and clinical significance of the candidate sgRNAs, the listed 1024 sgRNAs were translated into official gene symbols using DAVID, resulting into 995 candidate genes.

To link those potential markers of resistance with clinical data, we compared the candidate genes with genetic data from comprehensive analysis of muscle-invasive bladder cancers characterized by multiple TCGA analytical platforms on cBioPortal (Robertson et al., 2017). We filtered out the candidate genes without amplification in copy number alteration (CNA) since the functional relevance of most mutations has not been demonstrated. A panel of 882 genes was identified (Cerami et al., 2012; Gao et al., 2013; Power & Izawa, 2016). Analysis of integrative pathways with these genes were performed using Reactome pathway analysis, that identified distinct signaling pathways including cell cycle, DNA repair, programmed cell death, metabolism or signal transduction (Figure 15a). Targeting functional units of those pathways might overcome therapy resistance to monotherapy with Palbociclib. We also performed KEGG pathway analysis on DAVID, in which 'metabolism' and 'pathways in cancer' were most significantly overlapped with our candidate genes. Signaling pathways included in the term 'pathways in cancer' were analyzed for the availability of clinically applicable drugs using the database DGIdb (Cotto et al., 2017), which revealed several Receptor Tyrosine Kinases and the PI3K-AKT, Ras/MAPK, cell cycle and JAK-STAT pathway (Figure 15b).

Reactome pathway analysis

a

KEGG pathway analysis

b

Term	Count
hsa01100:Metabolic pathways	54
hsa05200:Pathways in cancer	22
hsa04144:Endocytosis	18
hsa04080:Neuroactive ligand-receptor interaction	16
hsa04810:Regulation of actin cytoskeleton	13
hsa01130:Biosynthesis of antibiotics	13
hsa05166:HTLV-I infection	13
hsa04390:Hippo signaling pathway	12
hsa05205:Proteoglycans in cancer	12
hsa04550:Signaling pathways regulating pluripotency of stem cells	10

Inhibitors/agonists	Target	Pathway
PIK-90	PI3Kα/γ/δ	PI3K-AKT
MK2206	Akt1/2/3	PI3K-AKT
Everolimus	mTOR	PI3K-AKT
NVP-BEZ235	p110α/γ/δ/β and mTOR	PI3K-AKT
Axitinib	VEGFR1/2/3, PDGFRβ and c-Kit	Ras/MAPK
Erdafitinib	FGFR1/2/3/4	Ras/MAPK
CI-1040	MEK1/2	Ras/MAPK
Ruxolitinib	JAK1/2	JAK-STAT
Stattic	STAT3	JAK-STAT
SH-4-54	STAT3/5	JAK-STAT
Roscovitine	CDK2/7/9	Cell cycle

Figure 15: Clinically actionably oncogenic signaling pathways analysis. a Reactome pathway analysis. **b** KEGG Pathway mapping with overlap of screen candidate genes and clinically amplified genes from cBioPortal. Inhibitors/agonists were selected from DGIdb.

4.2.7 Activation of identified pathway confer resistance to Palbociclib

To validate hyperactivation of those pathways with therapy resistance, genes with most frequently clinical amplification in bladder cancer including KDR, FGFR3, AKT3, JAK2, STAT3 were selected (Figure 16a). SgRNAs targeting above genes were transduced into T24 SAM cells and therapy response to Palbociclib was examined. Expression of all 5 sgRNAs and increase in the transcriptional level of target genes was confirmed (Figure 16b). The sgRNA transduced cells acquired resistance against Palbociclib, as

examined in cell viability and clonogenic assays conducted over 10 days when compared to NTC cells (Figure 16c,d).
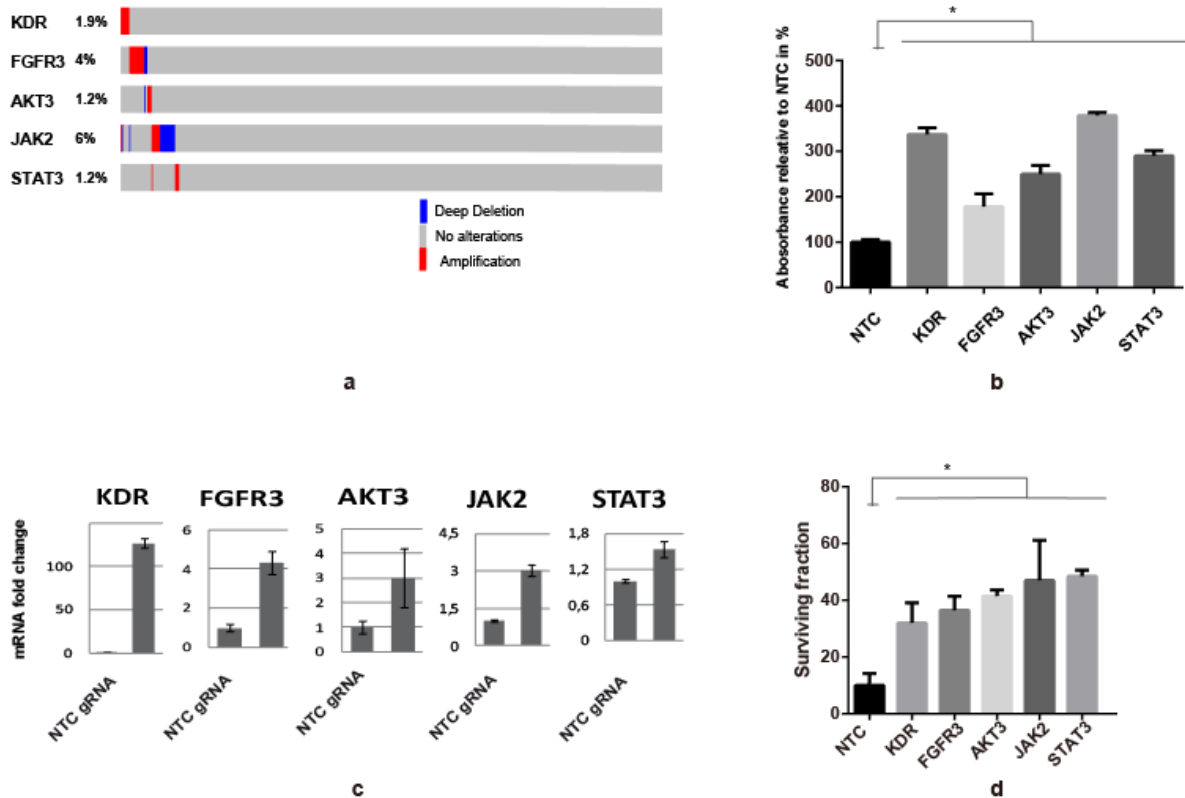
Figure 16: Validation for 5 candidate genes in multiple oncogenic signaling pathways. a Frequently amplified genes in bladder cancer belong to identified pathways. **b** Transcriptional activation of 5 candidate genes detected by qPCRs. **c** SRB cell proliferation assay after 4 days of Palbociclib (1000nM) treatment (*, P < 0.05; unpaired t-test compared to cells transduced with NTC gRNA). **d** 10 days clonogenic assay under Palbociclib (1000nM) results were counted, more than 50 cells were counted as a colony, surviving fraction= Colony number/Seeded cell number in % (*, P < 0.05; unpaired t-test compared to cells transduced with NTC gRNA). Data represent mean ± SD of 3 replicates.

4.3 Potential combination therapies were validated in vitro and a 3-dimensional tumor model

4.3.1 Synergistic combination therapies identified by CI analysis

Above results suggested that amplification of distinct pathways in bladder cancer can serve as indicators of resistance to Palbociclib. 11 inhibitors targeting the oncogenic signaling pathways identified above were applied to T24 and RT112 cells and

combined with Palbiciclib. Dose-response kinetics of these inhibitors/agonists and Palbociclib were performed in vitro in mono- and combination therapy and monitored for cell viability. With the Chou-Talalay method the combination index (CI) was calculated that revealed synergism for Palbociclib in combination with Axitinib, Erdafitinib, CI-1040, NVP-BEZ235, PIK90, MK2206, Rescovitine and Everolimus. The STAT inhibitors Stattic and SH-4-54 mainly showed additive effects. However, the JAK inhibitor Ruxolitinib showed antagonism(Figure 17a,b)[3].

RTK/PI3K-Akt pathway inhibitors and CDK2 inhibitors have been evaluated in combination with CDK4/6 inhibitors very detailed in other tumor entities before (Bonelli et al., 2017; Herrera-Abreu et al., 2016; Jansen et al., 2017; Vora et al., 2014). Thus, we focused on novel synergistic drug combinations with Axitinib, Erdafitinib, CI1040 and the PI3K/mTOR inhibitor NVP-BEZ235.

---

[3] This work was done together with Benedikt Ebner.
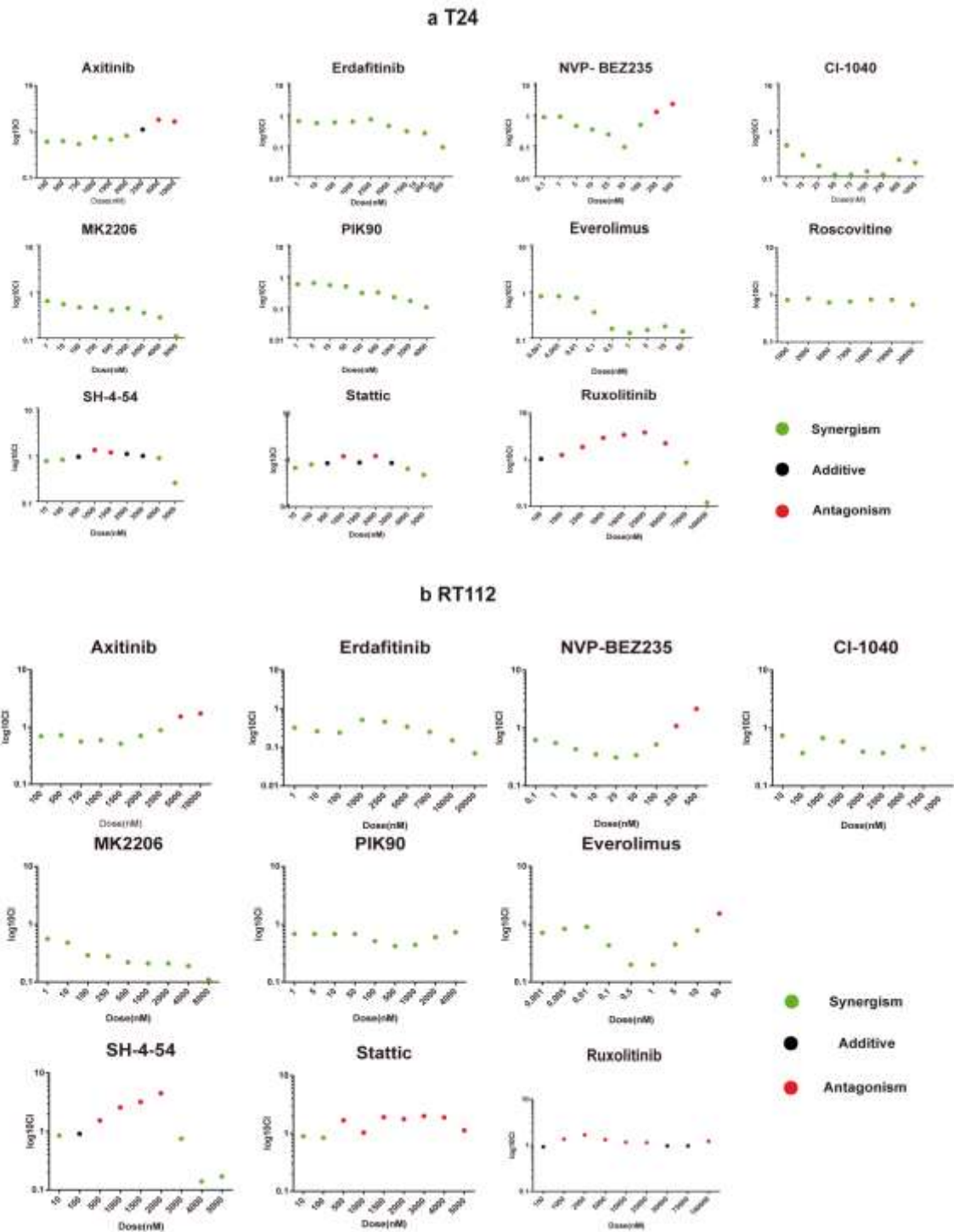
Figure 17: Combination Index analysis. Combination Index was calculated by 3 days CTB results under indicated treatments, and displaed with Log10 CI. **a** T24. **b** RT112

4.3.2 Synergism was detected in a 3-D xenograft model

To further evaluate the efficacy of combination therapies in a three-dimensional tumor

xenograft system, we used a RT112-luc xenograft model on the chicken chorioallantoic membrane (CAM) model because T24 cell xenografts in this model are very small. Response to Palbociclib was evaluated (Figure 6) and randomized to non-treated control and treatment with Palbociclib, Erdafitinib, Axitinib, CI-1040 or NVP-BEZ235 as mono- or combination therapy (Skowron et al., 2017). The combination therapies induced a statistically significant synergistic antitumor effect compared with monotherapies without increasing mortality of the developing chicken embryo (Figure 18)[4].
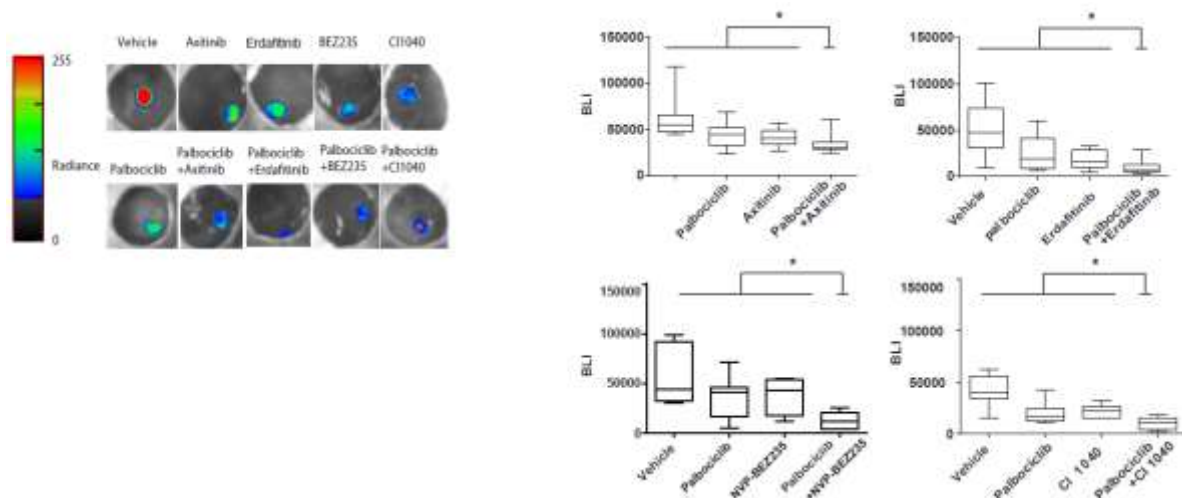
Figure 18: synergism evaluation in 3-dimensional culture on CAM system. CAM assays were performed with the RT112luc cell line and xenografts were treated 5 days with Palbociclib monotherapy or in combination with Axitinib, Erdafitinib, NVP-BEZ235, and CI1040 as above concentrations applied for 1ml blood volume. Luminescence intensity was measured as representation of viable cell numbers (*, $P < 0.05$; one-way ANOVA with Dunnett's multiple comparisons test, combination therapies compared to respective monotherapies and non-treated control).

4.4 Combination therapies overcome resistance to CDK4/6 inhibition via multiple molecular mechanisms

To unmask molecular mechanisms of acquired resistance to CDK4/6 inhibition and key effectors in combination therapies, we further detected relevant down-stream targets with Western blot. After Palbociclib treatment at 72H, p-ERK1/2, p-AKT, and p-p70s6k got hyper activated in both T24 and RT112 cell line, and this transition was in

---

[4] This work was done together with Benedikt Ebner.

synchronization with partial recovery of cell cycle progression. This might indicate that both PI3K and MAPK pathway activation contribute compensatory to the acquired resistance of CDK4/6 inhibition. Even in combination therapy with Palbociclib and BEZ235 in T24, p-ERK1/2, p-AKT still got hyper activated, an effect observed also for BEZ235 monotherapy (Sathe et al., 2018). Interestingly, blocking of the PI3K pathway downstream target p70s6k correlates with the achieved long-term anti-tumor activity (Figure 18,19).

We also observed increasing of CyclinD1 and p-CDK2 with Palbociclib monotherapy that could be reversed by combination therapies. In all combination therapies, we observed a persistent low level of p-RB andp-CDK2, indicating potential compensatory feedback loops were blocked and RB-E2F pathway got long-term blocked in combination therapies. Though in T24 cell line only CDK4/6 inhibition in combination with BEZ 235, almost zero level p-RB was detected. Low level of p-RB and p-cdk2 were consistent with better therapy response compared to Palbociclib monotherapy, so their status could be utilized as an indication of therapeutic efficiency during treatment.
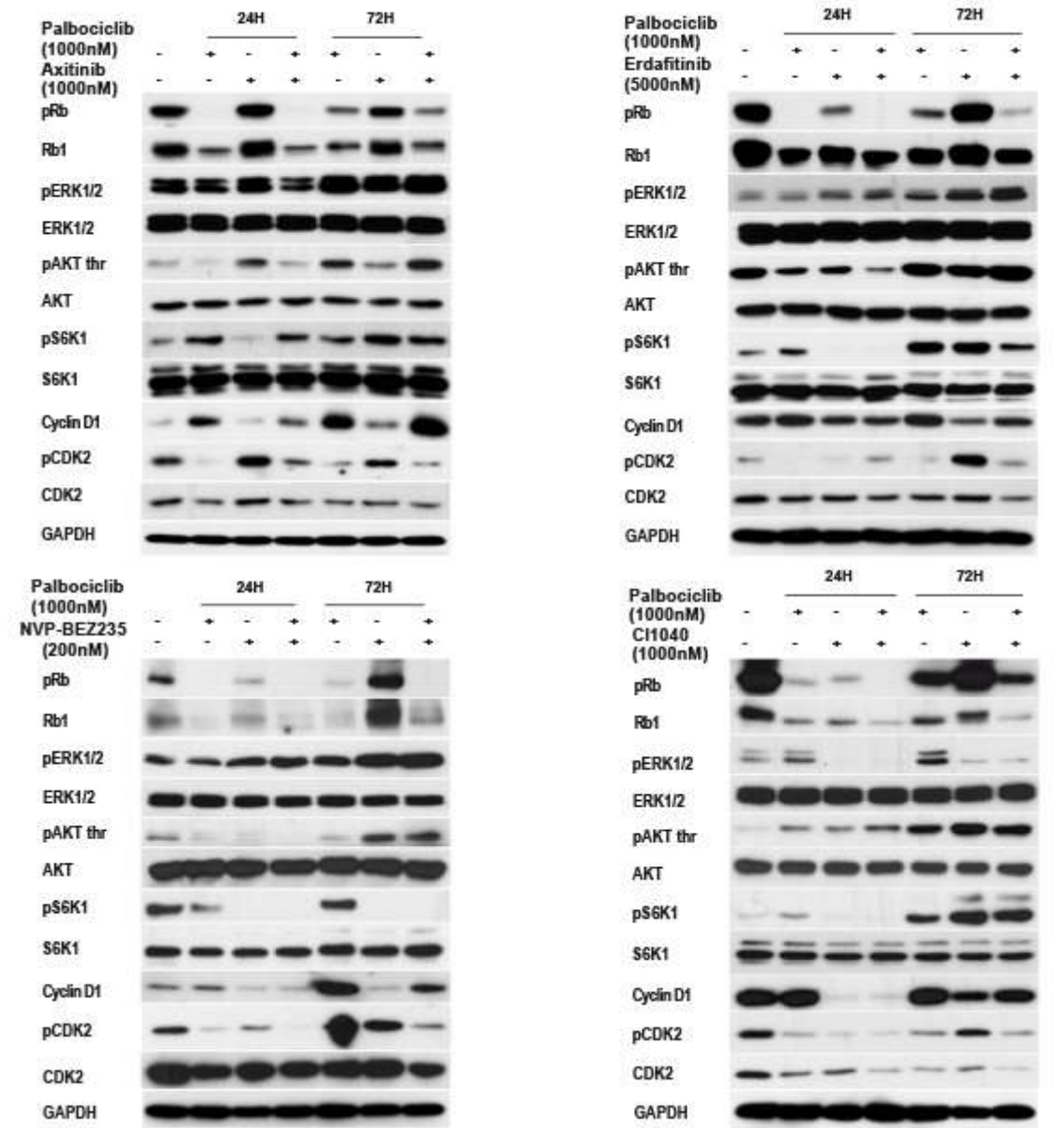
Figure 19: Western blot analysis revealed acquired resistance mechanism to CDK4/6 inhibition and molecular key components related to treatment efficacy on T24 cell line. The cells were lysed after indicated treatment and analyzed with WB of specific protein targets.
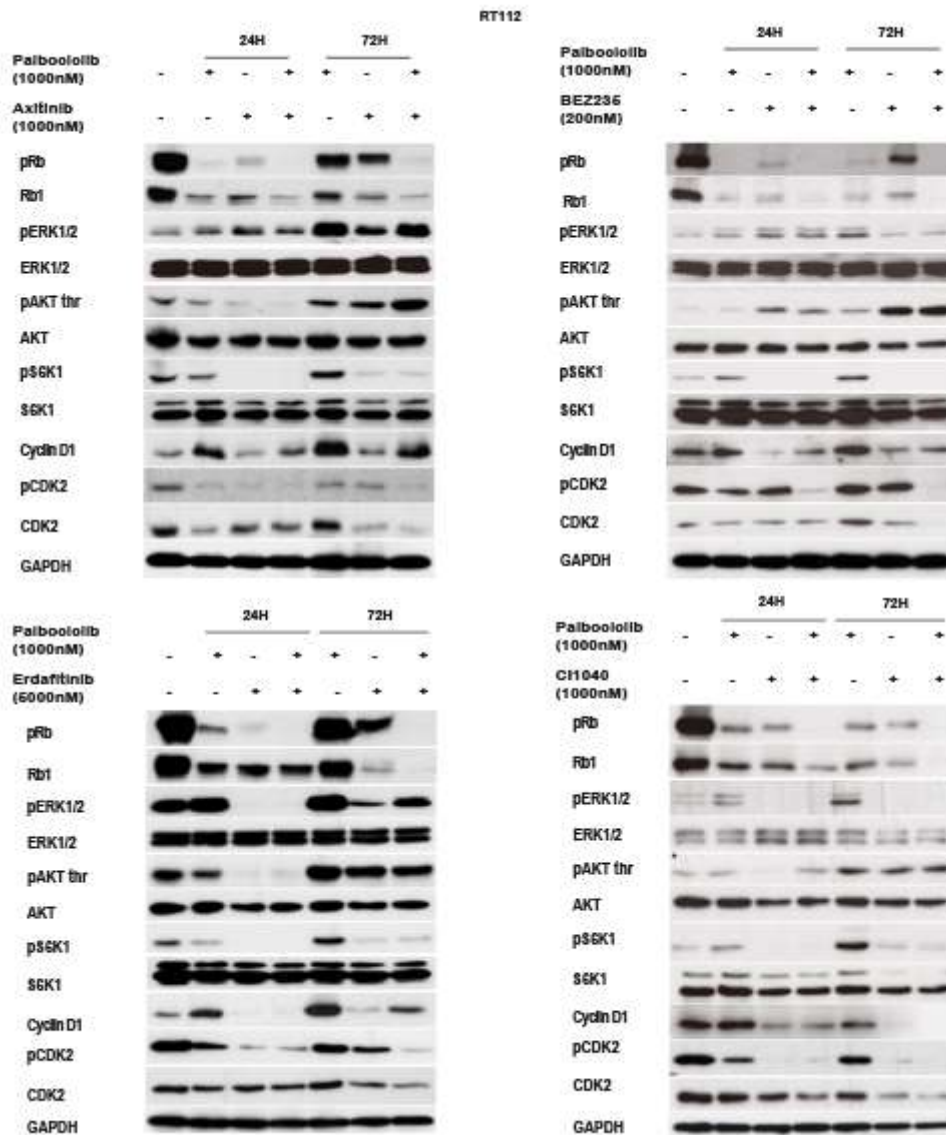
Figure 20: Western blot analysis revealed acquired resistance mechanism to CDK4/6 inhibition and molecular key components related to treatment efficacy on RT112 cell line. The cells were lysed after indicated treatment and analyzed with WB of specific protein targets.

4.5 Resistance to Palbociclib by transcriptional activation of KDR and FGFR3 can be reversed by application of combination therapies

A majority of bladder cancer specimen display mutations in signaling pathways that could be addressed with the above tested combination therapies (Robertson et al., 2017). We addressed the question if cells that exhibit overactivation of the respective pathways would be more susceptible to combination therapies using T24 SAM cells expressing sgRNAs for KDR and FGFR3. These cells exhibited resistance to Palbociclib and positive control Everolimus (mTORC1 inhibitor) monotherapy as

compared to NTC cells (Figure 20a) but responded equally to Erdafitinib or Axitinib respectively. When combining Palbociclib with either Axitinib or Erdafitinib, synergism could be observed and the induced resistance against Palbociclib monotherapy was eliminated in the respective cell lines (Fig 20a). Interestingly, the combination of Palbociclib and Everolimus did not act synergistically in these cells suggesting that patients with hyperactivated RTK would benefit better from a combination therapy that targets the amplified or hyperactivated kinase but not from a general downstream inhibitor.

4.6 Potential pre-stratification of bladder cancer patients to combination therapies

Based on above conclusion, we analyzed 412 bladder cancer patients from the TCGA dataset from cBioPortal and stratified these patients for the occurrence of deep deletion in RB1 and amplification in the candidate genes that belong to RTK, PI3K-Akt and Ras/MAPK signaling pathways. We found that 37 patients harbor RB1 deep deletion which means these patients would probably not benefit from a therapy that targets CDK4/6 (Figure 20b). 129 out of 412 patients have at least one gain of function mutation in the RTK, PI3K-Akt and Ras/MAPK signaling pathway. In accordance with above results, using Palbociclib in combination with inhibitors of these pathways may achieve a better anti-tumor effect. 246 patients did not show obvious mutations in the pathways analyzed and might also benefit from Palbociclib monotherapy.
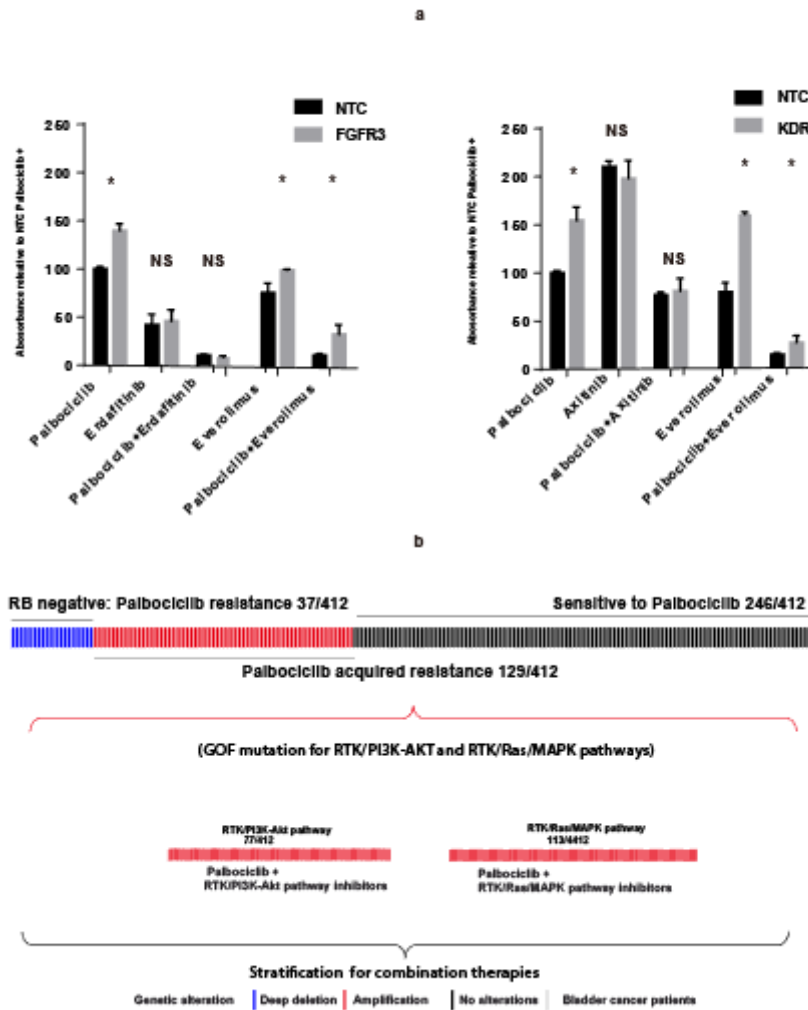
Figure 21: Efficiency of combination therapies on KDR and FGFR3 activation in T24 SAM cells and prediction of response to combination therapies on patients. a Efficiency of Palbociclib (1000nM) in combination with Axitinib (1000nM), Erdafitinib (5000nM), and Everolimus (5nM) was detected after 7 days' treatment on engineered T24 cells (*, $P < 0.05$; unpaired t-test with cells with KDR/FGFR3 gRNAs or NTC gRNA under respective treatment; NS not significant, Data represent mean ± SD of 3 replicates). **b** Pre-stratification of bladder cancer patients and prediction of response to combination therapies.

5 Discussion

Since mechanisms of acquired resistance to CDK4/6 inhibition in bladder cancer still are unclear, we aimed to reveal the mechanisms and further develop more efficient combination therapies. Thus, we performed a genome-scale CRISPR-dCas9 activation screen. By analyzing the NGS data of screen results obtained, we identified a panel of candidate sgRNAs which may confer resistance and by using informatics tools, we revealed a pathway network when activation may confer resistance. Then based on this result, we further developed several synergistic combination therapies. Although in an initial analysis, a panel of more than 1200 sgRNAs that were reduced in expression compared to the control, in this study only gain of sgRNAs was analyzed.

5.1 Potentiality and deficiency of using CRISPR/dCas9 as a tool for research of resistance mechanism

When using CRISPR/dCas9 high throughput technologies, off-target effects are always a major concern. For minimizing off-target effects induced by the sgRNAs design or genomic integration, the SAM library we used in this work was designed with minimal predicted off-target activity (Ran et al., 2013; Shalem et al., 2015). In addition, we used low-MOIs for transduction. The Pearson correlation coefficient between biological treatment replicates in our analysis was comparable to other CRISPR screen approaches that have a range from 0.25 – 0.92 overall (Han et al., 2018; Robertson et al., 2017). However, reproducibility among replicates remains a subject for improvement. We used one of the early systems developed but novel systems that were subsequently developed might overcome those potential limitations (Horlbeck et al., 2016; La Russa & Qi, 2015). When randomly chosen 8 significant candidate sgRNAs got biologically validated, we could demonstrated the practicality of CRISPR/dCas9 screen in research of the resistance mechanism.

5.2 Extension of understanding of resistance mechanism to CDK4/6 inhibition in bladder cancer

The clinically relevant question is, if identified oncogenic signaling molecules and pathways that induce an acquired resistance to CDK4/6 inhibitors can be targeted to overcome this resistance. Together with TCGA dataset, we revealed a range of different pathways with diverse biologic functions may confer resistance to CDK4/6 inhibitor. The diversity of different signaling events involved in the cellular response to CDK4/6 inhibitors reflect probably the diverse and complicated downstream signaling network of CDK4/6 as has been described only recently (Klein, Kovatcheva, Davis, Tap, & Koff, 2018; Knudsen & Witkiewicz, 2017). This diversity of molecular candidates

might also explain why the identification of one or at least few reliable predictive marker was not successful to date.

We extracted signaling pathways that are frequently mutated in bladder cancer patients and demonstrated that combinations with inhibitors targeting RTKs, PI3K-AKT and Ras/MAPK exhibited synergism with Palbociclib. Recently, resistance mechanisms to CDK4/6 inhibitors have been published by using different experimental approaches. For instance, a kinome-wide RNA interference, exome sequencing and a drug screen identified activation of the PI3K, JAK/STAT and MAPK pathway as mechanisms of acquired resistance and inhibitors against different key molecules in these pathways in breast cancer, myeloproliferative neoplasia, mucosal melanomas and Leukemia overcame this resistance (Herrera-Abreu et al., 2016; Jansen et al., 2017; Kim et al., 2017; Maria Pinzon-Ortiz, 2014). These results are in accordance with the results obtained from our CRISPR-dCas9 approach and link activation of multiple pathways to resistance to CDK4/6 inhibition (Pan et al., 2017). We also extended this knowledge by demonstrating that RTK inhibitors Axitinib and Erdafitinib showed synergism in combination. However, when combining inhibitors against JAK1/2 with Palbociclib, antagonistic effects were observed whereas STAT3/6 inhibitors acted additive. As monotherapy, bladder cancer cells do not respond to JAK inhibitors Ruxolitinib or BSK805 (data not shown), whereas STAT inhibitors are effective. We conclude from our data that the mechanism of action when using a CDK4/6 inhibitor is diverse and that a single pathway is only partially influencing therapy response. Also, cell cycle arrest and induced apoptosis contributed to the improved anti-tumor activity in combination therapies, but the genetic background of tumor cells significantly attributes to the level and direction of therapy response.

5.3 Potential stratification for CDK4/6 inhibition and combination therapies
Challenges in the design of clinical trials using CDK4/6 inhibitors are the molecular pre-stratification for mono- or combination therapy of patients according to their genetic background to achieve a maximum benefit (Dickler et al., 2017; Finn et al., 2016; Hortobagyi et al., 2016). Only RB1 expression has already been regarded as a promising biomarker in ongoing clinical trials. Cyclin D did not turn out as a reliable biomarker and transient inhibition of pRb with CDK4/6 inhibition has been demonstrated to be compensated by CDK2 (Gong et al., 2017; Pan et al., 2017). Activation of the PI3K/AKT pathway and coordinately activated CDK2 might represent potential biomarkers (Herrera-Abreu et al., 2016; Jansen et al., 2017). Based on these

preclinical findings, combination therapies in novel clinical trials among different tumor entities are ongoing (Medcine). As for improvement of patient stratification, we mimicked the genetic background of patients with defined activation of signaling pathways in bladder cancer. We genetically engineered a cell line that overexpressed KDR or FGFR3 which conferred resistance to Palbociclib monotherapy. Although T24 cells do harbor an activating Ras mutation our data indicate that a combination of CDK4/6 inhibitors paired with personalized inhibitors against one further pathway is beneficial for therapy and that identification of multiple activated pathways might open the option for a personalized sequential therapy. Our results together with published data indicate that a pre-stratification of patients for a personalized therapy approach is feasible.

6 Summary

Identification of molecular mechanisms of resistance to targeted therapies is a prerequisite for improving treatment efficacy by designing rational combination treatments and utilizing a personalized therapy approach. CDK4/6 inhibitors have shown their potency in the treatment of bladder cancer, but reliable markers to predict response and potential combination therapies are still missing.

We applied a combination of a forward genetic screen using the CRISPR-dCas9 technology and the analysis of large-scale cancer genomics data sets from patients to identify molecules and signaling pathways that confer resistance to the CDK4/6 inhibitor Palbociclib. We successfully amplified the SAM sgRNA library and generated a T24 SAM cell line. After infecting these cells with the sgRNA library, Palbociclib was applied in positively transduced cells to select for cells that would be resistant. Our screen was performed in a well-controled environment and reproducibility among all three replicates was acceptable based on quality control analysis of NGS data. By analyzing the NGS data of the screen, we identified 1024 positively enriched candidate sgRNAs and biologically validated 8 sgRNAs on transcriptional activation and further resistance to Palbociclib. With informatics tools, we identified not only molecules that are involved in therapy response to CDK4/6 monotherapy but also revealed a network of frequently mutated signaling pathways in patients that confer resistance together with our screen results. With further validation of frequently mutated genes that belong to these pathways by transcriptional activation with according sgRNAs, we demonstrated activation of these pathways may confer resistance to Palbociclib. Based on this finding, we designed several combination therapies and confirmed their long-term efficiency in vitro and 3-D xenograft model.

By analyzing the copy number alteration of patients from TCGA, we developed a model to stratify patients as for CDK4/6 monotherapy or proper combination therapies. Again, our findings highlight the diversity of the resistance mechanism to CDK4/6 inhibitors, instead of trying to find a potential one golden marker. A broader consideration of the genetic background of patients may be necessary to stratify into different treatment subgroups instead of responder vs non-responder .

In conclusion, we could demonstrate that use of a CRISPR-dCas9 genome scale gain of function screen for elucidating mechanisms of resistance to target therapies does reveal a dataset of candidate genes. We could validate that several signaling pathways

contribute to the resistance to CDK4/6 inhibiors but that suitable combination therapies can overcome this resistance. Together with TCGA dataset, that allows stratification of patients with distinct genetic pattern the design of suitable strategies for combination treatment to overcome potential resistance was developed. The application of CRISPR/dCas9 SAM system and corresponding sgRNAs library reveal better understanding of biological processes that are involved in signaling events related to specific drug targets.

Bibliography

Alfred Witjes, J., Lebret, T., Comperat, E. M., Cowan, N. C., De Santis, M., Bruins, H. M., . . . Ribal, M. J. (2017). Updated 2016 EAU Guidelines on Muscle-invasive and Metastatic Bladder Cancer. *Eur Urol, 71*(3), 462-475. doi:10.1016/j.eururo.2016.06.020

Andrews, S. (2010). FastQC: a quality control tool for high throughput sequence data. Retrieved from https://www.bioinformatics.babraham.ac.uk/projects/fastqc/

Bao, M., Wang, Y., Liu, Y., Shi, P., Lu, H., Sha, W., . . . Liu, Y. J. (2016). NFATC3 promotes IRF7 transcriptional activity in plasmacy--toid dendritic cells. *J Exp Med, 213*(11), 2383-2398. doi:10.1084/jem.20160438

Bellmunt, J., Powles, T., & Vogelzang, N. J. (2017). A review on the evolution of PD-1/PD-L1 immunotherapy for bladder cancer: The future is now. *Cancer Treat Rev, 54*, 58-67. doi:10.1016/j.ctrv.2017.01.007

Bonelli, M. A., Digiacomo, G., Fumarola, C., Alfieri, R., Quaini, F., Falco, A., . . . Petronini, P. G. (2017). Combined Inhibition of CDK4/6 and PI3K/AKT/mTOR Pathways Induces a Synergistic Anti-Tumor Effect in Malignant Pleural Mesothelioma Cells. *Neoplasia, 19*(8), 637-648. doi:10.1016/j.neo.2017.05.003

Bray, F., Ferlay, J., Soerjomataram, I., Siegel, R. L., Torre, L. A., & Jemal, A. (2018). Global cancer statistics 2018: GLOBOCAN estimates of incidence and mortality worldwide for 36 cancers in 185 countries. *CA Cancer J Clin*. doi:10.3322/caac.21492

Burger, M., Catto, J. W., Dalbagni, G., Grossman, H. B., Herr, H., Karakiewicz, P., . . . Lotan, Y. (2013). Epidemiology and risk factors of urothelial bladder cancer. *Eur Urol, 63*(2), 234-241. doi:10.1016/j.eururo.2012.07.033

Cerami, E., Gao, J., Dogrusoz, U., Gross, B. E., Sumer, S. O., Aksoy, B. A., . . . Schultz, N. (2012). The cBio cancer genomics portal: an open platform for exploring multidimensional cancer genomics data. *Cancer Discov, 2*(5), 401-404. doi:10.1158/2159-8290.CD-12-0095

Chamie, K., Ballon-Landa, E., Daskivich, T. J., Bassett, J. C., Lai, J., Hanley, J. M., . . . Urologic Diseases in America, P. (2015). Treatment and survival in patients with recurrent high-risk non-muscle-invasive bladder cancer. *Urol Oncol, 33*(1), 20 e29-20 e17. doi:10.1016/j.urolonc.2014.08.016

Choi, W., Porten, S., Kim, S., Willis, D., Plimack, E. R., Hoffman-Censits, J., . . . McConkey, D. J. (2014). Identification of distinct basal and luminal subtypes of muscle-invasive bladder cancer with different sensitivities to frontline chemotherapy. *Cancer Cell, 25*(2), 152-165. doi:10.1016/j.ccr.2014.01.009

Chou, T. C. (2006). Theoretical basis, experimental design, and computerized simulation of synergism and antagonism in drug combination studies. *Pharmacol Rev, 58*(3), 621-681. doi:10.1124/pr.58.3.10

Cotto, K. C., Wagner, A. H., Feng, Y. Y., Kiwala, S., Coffman, A. C., Spies, G., . . . Griffith, M. (2017). DGIdb 3.0: a redesign and expansion of the drug-gene interaction database. *Nucleic Acids Res*. doi:10.1093/nar/gkx1143

Dadhania, V., Zhang, M., Zhang, L., Bondaruk, J., Majewski, T., Siefker-Radtke, A., . . . Czerniak, B. (2016). Meta-Analysis of the Luminal and Basal Subtypes of Bladder Cancer and the Identification of Signature Immunohistochemical Markers for Clinical Use. *EBioMedicine, 12*, 105-117. doi:10.1016/j.ebiom.2016.08.036

Dickler, M. N., Tolaney, S. M., Rugo, H. S., Cortes, J., Dieras, V., Patt, D., . . . Baselga, J. (2017). MONARCH 1, A Phase II Study of Abemaciclib, a CDK4 and CDK6 Inhibitor, as a Single Agent, in Patients with Refractory HR(+)/HER2(-) Metastatic Breast Cancer. *Clin Cancer Res, 23*(17), 5218-5224. doi:10.1158/1078-0432.CCR-17-0754

Doudna, J. A., & Charpentier, E. (2014). Genome editing. The new frontier of genome engineering with CRISPR-Cas9. *Science, 346*(6213), 1258096. doi:10.1126/science.1258096

Eisenberg, E., & Levanon, E. Y. (2013). Human housekeeping genes, revisited. *Trends Genet, 29*(10), 569-574. doi:10.1016/j.tig.2013.05.010

Fabregat, A., Jupe, S., Matthews, L., Sidiropoulos, K., Gillespie, M., Garapati, P., . . . D'Eustachio, P. (2018). The Reactome Pathway Knowledgebase. *Nucleic Acids Res, 46*(D1), D649-D655. doi:10.1093/nar/gkx1132

Finn, R. S., Martin, M., Rugo, H. S., Jones, S., Im, S. A., Gelmon, K., . . . Slamon, D. J. (2016). Palbociclib and Letrozole in Advanced Breast Cancer. *N Engl J Med, 375*(20), 1925-1936. doi:10.1056/NEJMoa1607303

Franken, N. A., Rodermond, H. M., Stap, J., Haveman, J., & van Bree, C. (2006). Clonogenic assay of cells in vitro. *Nat Protoc, 1*(5), 2315-2319. doi:10.1038/nprot.2006.339

Gao, J., Aksoy, B. A., Dogrusoz, U., Dresdner, G., Gross, B., Sumer, S. O., . . . Schultz, N. (2013). Integrative analysis of complex cancer genomics and clinical profiles using the cBioPortal. *Sci Signal, 6*(269), pl1. doi:10.1126/scisignal.2004088

Gebre, M., Nomburg, J. L., & Gewurz, B. E. (2018). CRISPR-Cas9 Genetic Analysis of Virus-Host Interactions. *Viruses, 10*(2). doi:10.3390/v10020055

Gilbert, L. A., Horlbeck, M. A., Adamson, B., Villalta, J. E., Chen, Y., Whitehead, E. H., . . . Weissman, J. S. (2014). Genome-Scale CRISPR-Mediated Control of Gene Repression and Activation. *Cell, 159*(3), 647-661. doi:10.1016/j.cell.2014.09.029

Gong, X., Litchfield, L. M., Webster, Y., Chio, L. C., Wong, S. S., Stewart, T. R., . . . Buchanan, S. G. (2017). Genomic Aberrations that Activate D-type Cyclins Are Associated with Enhanced Sensitivity to the CDK4 and CDK6 Inhibitor Abemaciclib. *Cancer Cell, 32*(6), 761-776 e766. doi:10.1016/j.ccell.2017.11.006

Guarducci, C., Bonechi, M., Boccalini, G., Benelli, M., Risi, E., Di Leo, A., . . . Migliaccio, I. (2017). Mechanisms of Resistance to CDK4/6 Inhibitors in Breast Cancer and Potential Biomarkers of Response. *Breast Care (Basel), 12*(5), 304-308. doi:10.1159/000484167

Guo, C. C., Dadhania, V., Zhang, L., Majewski, T., Bondaruk, J., Sykulski, M., . . . Czerniak, B. (2016). Gene Expression Profile of the Clinically Aggressive Micropapillary Variant of Bladder Cancer. *Eur Urol, 70*(4), 611-620. doi:10.1016/j.eururo.2016.02.056

Han, J., Perez, J. T., Chen, C., Li, Y., Benitez, A., Kandasamy, M., . . . Manicassamy, B. (2018). Genome-wide CRISPR/Cas9 Screen Identifies Host Factors Essential for Influenza Virus Replication. *Cell Rep, 23*(2), 596-607. doi:10.1016/j.celrep.2018.03.045

Herrera-Abreu, M. T., Palafox, M., Asghar, U., Rivas, M. A., Cutts, R. J., Garcia-Murillas, I., . . . Serra, V. (2016). Early Adaptation and Acquired Resistance to CDK4/6 Inhibition in Estrogen Receptor-Positive Breast Cancer. *Cancer Res, 76*(8), 2301-2313. doi:10.1158/0008-5472.CAN-15-0728

Horlbeck, M. A., Gilbert, L. A., Villalta, J. E., Adamson, B., Pak, R. A., Chen, Y., . . . Weissman, J. S. (2016). Compact and highly active next-generation libraries for CRISPR-mediated gene repression and activation. *Elife, 5*. doi:10.7554/eLife.19760

Hortobagyi, G. N., Stemmer, S. M., Burris, H. A., Yap, Y. S., Sonke, G. S., Paluch-Shimon, S., . . . O'Shaughnessy, J. (2016). Ribociclib as First-Line Therapy for HR-Positive, Advanced Breast Cancer. *N Engl J Med, 375*(18), 1738-1748. doi:10.1056/NEJMoa1609709

Huang da, W., Sherman, B. T., & Lempicki, R. A. (2009). Systematic and integrative analysis of large gene lists using DAVID bioinformatics resources. *Nat Protoc, 4*(1), 44-57. doi:10.1038/nprot.2008.211

Humphrey, P. A., Moch, H., Cubilla, A. L., Ulbright, T. M., & Reuter, V. E. (2016). The 2016 WHO Classification of Tumours of the Urinary System and Male Genital Organs-Part B: Prostate and Bladder Tumours. *Eur Urol, 70*(1), 106-119. doi:10.1016/j.eururo.2016.02.028

Infante, J. R., Cassier, P. A., Gerecitano, J. F., Witteveen, P. O., Chugh, R., Ribrag, V., . . . Shapiro, G. I. (2016). A Phase I Study of the Cyclin-Dependent Kinase 4/6 Inhibitor Ribociclib (LEE011) in Patients with Advanced Solid Tumors and Lymphomas. *Clin Cancer Res, 22*(23), 5696-5705. doi:10.1158/1078-0432.CCR-16-1248

Iwata, H. (2018). Clinical development of CDK4/6 inhibitor for breast cancer. *Breast Cancer*. doi:10.1007/s12282-017-0827-3

Jansen, V. M., Bhola, N. E., Bauer, J. A., Formisano, L., Lee, K. M., Hutchinson, K. E., . . . Arteaga, C. L. (2017). Kinome-Wide RNA Interference Screen Reveals a Role for PDK1 in Acquired Resistance to CDK4/6 Inhibition in ER-Positive Breast Cancer. *Cancer Res, 77*(9), 2488-2499. doi:10.1158/0008-5472.CAN-16-2653

Kim, H. S., Jung, M., Kang, H. N., Kim, H., Park, C. W., Kim, S. M., . . . Cho, B. C. (2017). Oncogenic BRAF fusions in mucosal melanomas activate the MAPK pathway and are sensitive to MEK/PI3K inhibition or MEK/CDK4/6 inhibition. *Oncogene, 36*(23), 3334-3345. doi:10.1038/onc.2016.486

Klein, M. E., Kovatcheva, M., Davis, L. E., Tap, W. D., & Koff, A. (2018). CDK4/6 Inhibitors: The Mechanism of Action May Not Be as Simple as Once Thought. *Cancer Cell, 34*(1), 9-20. doi:10.1016/j.ccell.2018.03.023

Knowles, M. A., & Hurst, C. D. (2015). Molecular biology of bladder cancer: new insights into pathogenesis and clinical diversity. *Nat Rev Cancer, 15*(1), 25-41. doi:10.1038/nrc3817

Knudsen, E. S., & Witkiewicz, A. K. (2017). The Strange Case of CDK4/6 Inhibitors: Mechanisms, Resistance, and Combination Strategies. *Trends Cancer, 3*(1), 39-55. doi:10.1016/j.trecan.2016.11.006

Konermann, S., Brigham, M. D., Trevino, A. E., Joung, J., Abudayyeh, O. O., Barcena, C., . . . Zhang, F. (2015). Genome-scale transcriptional activation by an engineered CRISPR-Cas9 complex. *Nature, 517*(7536), 583-588. doi:10.1038/nature14136

La Russa, M. F., & Qi, L. S. (2015). The New State of the Art: Cas9 for Gene Activation and Repression. *Mol Cell Biol, 35*(22), 3800-3809. doi:10.1128/MCB.00512-15

Li, W., Koster, J., Xu, H., Chen, C. H., Xiao, T., Liu, J. S., . . . Liu, X. S. (2015). Quality control, modeling, and visualization of CRISPR screens with MAGeCK-VISPR. *Genome Biol, 16*, 281. doi:10.1186/s13059-015-0843-6

Li, W., Xu, H., Xiao, T., Cong, L., Love, M. I., Zhang, F., . . . Liu, X. S. (2014). MAGeCK enables robust identification of essential genes from genome-scale CRISPR/Cas9 knockout screens. *Genome Biol, 15*(12), 554. doi:10.1186/s13059-014-0554-4

Livak, K. J., & Schmittgen, T. D. (2001). Analysis of relative gene expression data using real-time quantitative PCR and the 2(-Delta Delta C(T)) Method. *Methods, 25*(4), 402-408. doi:10.1006/meth.2001.1262

Maria Pinzon-Ortiz, X. R., Abdel Saci, Robert Schlegel, Gary Vanasse, Giordano Caponigro and Z. Alexander Cao. (2014). *Abstract 3684: The combination of JAK inhibitor, ruxolitinib, pan-PIM inhibitor, LGH447, and CDK4/6 inhibitor, LEE011, in a preclinical mouse model of myeloproliferative neoplasia.* Paper presented at the AACR Annual Meeting 2014, San Diego, CA.

Cutadapt removes adapter sequences from high-throughput sequencing reads., 17 C.F.R. (2011).

Medcine, U. S. N. L. o.   Retrieved from https://clinicaltrials.gov/

Mohammed, A. A., El-Tanni, H., El-Khatib, H. M., Mirza, A. A., Mirza, A. A., & Alturaifi, T. H. (2016). Urinary Bladder Cancer: Biomarkers and Target Therapy, New Era for More Attention. *Oncol Rev, 10*(2), 320. doi:10.4081/oncol.2016.320

Mortality, G. B. D., & Causes of Death, C. (2016). Global, regional, and national life expectancy, all-cause mortality, and cause-specific mortality for 249 causes of death, 1980-2015: a systematic analysis for the Global Burden of Disease Study 2015. *Lancet, 388*(10053), 1459-1544. doi:10.1016/S0140-6736(16)31012-1

Nawroth, R., van Zante, A., Cervantes, S., McManus, M., Hebrok, M., & Rosen, S. D. (2007). Extracellular sulfatases, elements of the Wnt signaling pathway, positively regulate growth and tumorigenicity of human pancreatic cancer cells. *PLoS One, 2*(4), e392. doi:10.1371/journal.pone.0000392

Pan, Q., Sathe, A., Black, P. C., Goebell, P. J., Kamat, A. M., Schmitz-Draeger, B., & Nawroth, R. (2017). CDK4/6 Inhibitors in Cancer Therapy: A Novel Treatement Strategy for Bladder Cancer. *Bladder Cancer, 3*(2), 79-88. doi:10.3233/BLC-170105

Patnaik, A., Rosen, L. S., Tolaney, S. M., Tolcher, A. W., Goldman, J. W., Gandhi, L., . . . Shapiro, G. I. (2016). Efficacy and Safety of Abemaciclib, an Inhibitor of CDK4 and CDK6, for Patients with Breast Cancer, Non-Small Cell Lung Cancer, and Other Solid Tumors. *Cancer Discov, 6*(7), 740-753. doi:10.1158/2159-8290.CD-16-0095

Petrylak, D. P., Tangen, C. M., Van Veldhuizen, P. J., Jr., Goodwin, J. W., Twardowski, P. W., Atkins, J. N., . . . Crawford, E. D. (2010). Results of the Southwest Oncology Group phase II evaluation (study S0031) of ZD1839 for advanced transitional cell carcinoma of the urothelium. *BJU Int, 105*(3), 317-321. doi:10.1111/j.1464-410X.2009.08799.x

Pettenati, C., & Ingersoll, M. A. (2018). Mechanisms of BCG immunotherapy and its outlook for bladder cancer. *Nat Rev Urol, 15*(10), 615-625. doi:10.1038/s41585-018-0055-4

Power, N. E., & Izawa, J. (2016). Comparison of Guidelines on Non-Muscle Invasive Bladder Cancer (EAU, CUA, AUA, NCCN, NICE). *Bladder Cancer, 2*(1), 27-36. doi:10.3233/BLC-150034

Ran, F. A., Hsu, P. D., Lin, C. Y., Gootenberg, J. S., Konermann, S., Trevino, A. E., . . . Zhang, F. (2013). Double nicking by RNA-guided CRISPR Cas9 for enhanced genome editing specificity. *Cell, 154*(6), 1380-1389. doi:10.1016/j.cell.2013.08.021

Robertson, A. G., Kim, J., Al-Ahmadie, H., Bellmunt, J., Guo, G., Cherniack, A. D., . . . Lerner, S. P. (2017). Comprehensive Molecular Characterization of Muscle-Invasive Bladder Cancer. *Cell, 171*(3), 540-556 e525. doi:10.1016/j.cell.2017.09.007

Robertson, A. G., Kim, J., Al-Ahmadie, H., Bellmunt, J., Guo, G., Cherniack, A. D., . . . Lerner, S. P. (2018). Comprehensive Molecular Characterization of Muscle-Invasive Bladder Cancer. *Cell, 174*(4), 1033. doi:10.1016/j.cell.2018.07.036

Sanjana, N. E., Shalem, O., & Zhang, F. (2014). Improved vectors and genome-wide libraries for CRISPR screening. *Nat Methods, 11*(8), 783-784. doi:10.1038/nmeth.3047

Sanli, O., Dobruch, J., Knowles, M. A., Burger, M., Alemozaffar, M., Nielsen, M. E., & Lotan, Y. (2017). Bladder cancer. *Nat Rev Dis Primers, 3*, 17022. doi:10.1038/nrdp.2017.22

Sathe, A., Chalaud, G., Oppolzer, I., Wong, K. Y., von Busch, M., Schmid, S. C., . . . Nawroth, R. (2018). Parallel PI3K, AKT and mTOR inhibition is required to control feedback loops that limit tumor therapy. *PLoS One, 13*(1), e0190854. doi:10.1371/journal.pone.0190854

Sathe, A., Koshy, N., Schmid, S. C., Thalgott, M., Schwarzenbock, S. M., Krause, B. J., . . . Nawroth, R. (2016). CDK4/6 Inhibition Controls Proliferation of Bladder Cancer and Transcription of RB1. *J Urol, 195*(3), 771-779. doi:10.1016/j.juro.2015.08.082

Seiler, R., Ashab, H. A. D., Erho, N., van Rhijn, B. W. G., Winters, B., Douglas, J., . . . Black, P. C. (2017). Impact of Molecular Subtypes in Muscle-invasive Bladder Cancer on Predicting Response and Survival after Neoadjuvant Chemotherapy. *Eur Urol, 72*(4), 544-554. doi:10.1016/j.eururo.2017.03.030

Shalem, O., Sanjana, N. E., & Zhang, F. (2015). High-throughput functional genomics using CRISPR-Cas9. *Nat Rev Genet, 16*(5), 299-311. doi:10.1038/nrg3899

Skowron, M. A., Sathe, A., Romano, A., Hoffmann, M. J., Schulz, W. A., van Koeveringe, G. A., . . . Niegisch, G. (2017). Applying the chicken embryo chorioallantoic membrane assay to study treatment approaches in urothelial carcinoma. *Urol Oncol, 35*(9), 544 e511-544 e523. doi:10.1016/j.urolonc.2017.05.003

Smith, A. B., Deal, A. M., Woods, M. E., Wallen, E. M., Pruthi, R. S., Chen, R. C., . . . Nielsen, M. E. (2014). Muscle-invasive bladder cancer: evaluating treatment and survival in the National Cancer Data Base. *BJU Int, 114*(5), 719-726. doi:10.1111/bju.12601

Vora, S. R., Juric, D., Kim, N., Mino-Kenudson, M., Huynh, T., Costa, C., . . . Engelman, J. A. (2014). CDK 4/6 inhibitors sensitize PIK3CA mutant breast cancer to PI3K inhibitors. *Cancer Cell, 26*(1), 136-149. doi:10.1016/j.ccr.2014.05.020

Wang, L., Saci, A., Szabo, P. M., Chasalow, S. D., Castillo-Martin, M., Domingo-Domenech, J., . . . Galsky, M. D. (2018). EMT- and stroma-related gene expression and resistance to PD-1 blockade in urothelial cancer. *Nat Commun, 9*(1), 3503. doi:10.1038/s41467-018-05992-x

Willis, D., & Kamat, A. M. (2015). Nonurothelial bladder cancer and rare variant histologies. *Hematol Oncol Clin North Am, 29*(2), 237-252, viii. doi:10.1016/j.hoc.2014.10.011

Witjes, J. A., Comperat, E., Cowan, N. C., De Santis, M., Gakis, G., Lebret, T., . . . European Association of, U. (2014). EAU guidelines on muscle-invasive and metastatic bladder cancer: summary of the 2013 guidelines. *Eur Urol, 65*(4), 778-792. doi:10.1016/j.eururo.2013.11.046

Appendix
Table 14: significant candidate sgRNAs, rank with FDR.

rank	sgRNA ID	rank	sgRNA ID	rank	sgRNA ID	rank	sgRNA ID
1	NM_000458_1073	78	NM_014165_42960	155	NM_001005366_3544	232	NM_147150_62315
2	NM_001130996_10950	79	NM_003931_34159	156	NM_138401_60492	233	NM_005720_37980
3	NM_013441_42667	80	NM_020964_51727	157	NM_014500_43639	234	NM_001258454_23096
4	NM_016053_46384	81	NM_020696_51198	158	NM_024698_54509	235	NM_001077397_7085
5	NM_174922_65519	82	NM_021136_52030	159	NM_001039538_6161	236	NM_207009_69759
6	NM_012293_41863	83	NM_001191013_17886	160	NM_001252197_21743	237	NM_001276264_24223
7	NM_001267606_23387	84	NM_001018072_5131	161	NM_198567_68577	238	NM_001285486_26505
8	NM_145028_61748	85	NM_001278279_24700	162	NM_002222_30368	239	NM_024848_54803
9	NM_213649_70262	86	NM_006562_39793	163	NM_001135554_11404	240	NM_001860_29526
10	NM_004831_36003	87	NM_001145295_13410	164	NM_001017973_5054	241	NM_001139441_12013
11	NM_172070_64574	88	NM_052899_58861	165	NM_194272_67905	242	NM_016002_46280
12	NM_181713_67037	89	NM_005534_37583	166	NM_015908_46086	243	NM_199121_68883
13	NM_001142595_12383	90	NM_052885_58833	167	NM_005046_36475	244	NM_001206654_20220
14	NM_014619_43820	91	NM_020894_51608	168	NM_001025091_5348	245	NM_001178031_17168
15	NM_001033930_5799	92	NM_001174153_16997	169	NM_001278482_24854	246	NM_001136036_11686
16	NM_033071_58051	93	NM_003244_32650	170	NM_199337_69032	247	NM_001271831_24002
17	NM_001127386_10036	94	NM_001085399_8035	171	NM_001278579_24949	248	NM_001080521_7678
18	NM_005982_38541	95	NM_015414_45445	172	NM_173660_65232	249	NM_015676_45875
19	NM_001483_28716	96	NM_022787_53417	173	NM_001005366_3546	250	NM_007033_40789
20	NM_205843_69571	97	NM_001242913_21002	174	NM_020789_51396	251	NM_033647_58679
21	NM_000025_30	98	NM_031372_56033	175	NM_005348_37163	252	NM_152411_62833
22	NM_004625_35573	99	NM_024701_54515	176	NM_006937_40586	253	NM_001375_28504
23	NM_138804_60882	100	NM_001797_29373	177	NM_001243942_21442	254	NM_213604_70235
24	NM_014059_42848	101	NM_001184788_17402	178	NM_001204056_19785	255	NM_001193270_17957
25	NM_014141_42924	102	NM_145047_61783	179	NM_032937_57853	256	NM_001039762_6253
26	NM_001277304_24458	103	NM_033015_57944	180	NM_001142807_12524	257	NM_001004_2770
27	NM_025059_55071	104	NM_006042_38672	181	NM_002583_31182	258	NM_181575_66876
28	NM_016111_46504	105	NM_024086_53866	182	NM_001286559_26816	259	NM_001204144_19842
29	NM_017436_47571	106	NM_015950_46170	183	NM_033414_58500	260	NM_002263_30460
30	NM_004494_35290	107	NM_022556_53236	184	NM_152788_63573	261	NM_007144_40984
31	NM_032882_57793	108	NM_001287755_27362	185	NM_019892_50461	262	NM_017810_48174
32	NM_024418_54078	109	NM_173573_65107	186	NM_024681_54471	263	NM_006593_39865
33	NM_001312_28386	110	NM_014957_44552	187	NM_001128208_10296	264	NM_014638_43865
34	NM_000538_1244	111	NM_201559_69225	188	NM_005080_36561	265	NM_006534_39727
35	NM_001271822_23989	112	NM_001282428_25607	189	NM_017854_48281	266	NM_022821_53446
36	NM_020134_50540	113	NM_001099285_8497	190	NM_015871_46020	267	NM_002563_31133
37	NM_001134363_11032	114	NM_004117_34516	191	NM_001244015_21460	268	NM_001278284_24708
38	NM_002252_30432	115	NM_001166698_15704	192	NM_001204375_19951	269	NM_016226_46699

39	NM_013397_42622	116	NM_001287810_27375	193	NM_001243745_21359	270	NM_014059_42847
40	NM_001168393_15998	117	NM_173552_65060	194	NM_178438_66392	271	NM_001127203_9930
41	NM_005982_38542	118	NM_005254_36937	195	NM_006560_39786	272	NM_018156_48878
42	NM_138959_60919	119	NM_021147_52056	196	NM_001018024_5109	273	NM_001161657_14609
43	NM_015443_45504	120	NM_002757_31557	197	NM_001286810_27057	274	NM_001258328_22986
44	NM_001282403_25566	121	NM_015177_45009	198	NM_052853_58769	275	NM_022094_52802
45	NM_001242525_20737	122	NM_003413_33040	199	NM_003508_33224	276	NM_001013632_4700
46	NM_001150_14159	123	NM_001037163_5908	200	NM_024334_54044	277	NM_014339_43305
47	NM_080660_59561	124	NM_001195102_18294	201	NM_001160224_14433	278	NM_001720_29190
48	NM_007231_41160	125	NM_015261_45158	202	NM_001008388_3982	279	NM_000252_557
49	NM_018411_49397	126	NM_001001330_2236	203	NM_013327_42478	280	NM_205856_69595
50	NM_001662_29058	127	NM_015650_45828	204	NM_015621_45781	281	NM_001207037_20448
51	NM_003467_33135	128	NM_001198569_18712	205	NM_022170_52979	282	NM_021640_52360
52	NM_000891_1966	129	NM_033504_58589	206	NM_001271854_24028	283	NM_001042573_6738
53	NM_032189_56644	130	NM_199340_69038	207	NM_004102_34482	284	NM_007147_40991
54	NM_018053_48659	131	NM_000146_300	208	NM_001098626_8355	285	NM_004962_36278
55	NM_198992_68825	132	NM_001142482_12290	209	NM_025264_55390	286	NM_006703_40095
56	NM_001042545_6723	133	NM_005025_36428	210	NM_001256505_22332	287	NM_198699_68676
57	NM_001085411_8042	134	NM_001042693_6800	211	NM_018622_49607	288	NM_015984_46247
58	NM_001127668_10166	135	NM_014023_42786	212	NM_001098537_8321	289	NM_001135586_11424
59	NM_004781_35900	136	NM_021079_51932	213	NM_033020_57953	290	NM_001099652_8592
60	NM_001243718_21335	137	NM_001282406_25574	214	NM_001204265_19910	291	NM_004423_35137
61	NM_004043_34353	138	NM_198527_68511	215	NM_000437_1018	292	NM_001144897_12976
62	NM_017649_47878	139	NM_001265593_23275	216	NM_173810_65334	293	NM_001034_5807
63	NM_001042402_6604	140	NM_001100167_8739	217	NM_003281_32745	294	NM_001943_29715
64	NM_138396_60487	141	NM_018419_49413	218	NM_001282236_25461	295	NM_023067_53603
65	NM_001278411_24816	142	NM_001109662_9230	219	NM_001286_26523	296	NM_001136001_11633
66	NM_003453_33108	143	NM_003934_34164	220	NM_015889_46049	297	NM_015015_44664
67	NM_207352_69936	144	NM_001080439_7475	221	NM_004705_35748	298	NM_024940_54933
68	NM_006214_39021	145	NM_001113525_9479	222	NM_031283_55961	299	NM_004178_34646
69	NM_001242484_20712	146	NM_015104_44860	223	NM_001164232_14916	300	NM_133180_60019
70	NM_003172_32516	147	NM_101395_59818	224	NM_001204889_20093	301	NM_033276_58340
71	NM_001199184_19070	148	NM_148896_62413	225	NM_203464_69509	302	NM_001005368_3548
72	NM_021228_52220	149	NM_170696_64425	226	NM_152735_63464	303	NM_173199_64814
73	NM_002833_31734	150	NM_001142392_12206	227	NM_015193_45047	304	NM_171982_64526
74	NM_022773_53392	151	NM_001272050_24158	228	NM_001127641_10142	305	NM_199336_69028
75	NM_198316_68273	152	NM_153442_64086	229	NM_015516_45639	306	NM_002990_32084
76	NM_006547_39758	153	NM_001135655_11468	230	NM_001242874_20970	307	NM_005235_36891
77	NM_001015887_4916	154	NM_021047_51870	231	NM_001083592_7937	308	NM_002026_29899

rank	sgRNA ID	rank	sgRNA ID	rank	sgRNA ID	rank	sgRNA ID
309	NM_006290_39191	386	NM_000574_1318	463	NM_003769_33804	540	NM_207370_69973
310	NM_020441_50979	387	NM_001164883_15246	464	NM_004518_35337	541	NM_002849_31768
311	NM_001198869_18867	388	NM_018253_49075	465	NM_031904_56258	542	NM_003256_32684
312	NM_002809_31680	389	NM_001965_29766	466	NM_152908_63683	543	NM_170776_64506
313	NM_001146334_14102	390	NM_001080512_7655	467	NM_001130820_10854	544	NM_012259_41785
314	NM_173683_65262	391	NM_000913_2011	468	NM_001146152_13989	545	NM_001015072_4898
315	NM_003054_32253	392	NM_020337_50791	469	NM_212554_70183	546	NM_001077663_7159
316	NM_152434_62884	393	NM_001145132_13264	470	NM_014353_43333	547	NM_139277_61145
317	NM_001040663_6529	394	NM_001190811_17791	471	NM_001170794_16255	548	NM_001102398_8946
318	NM_016540_47236	395	NM_004775_35886	472	NM_001198868_18865	549	NM_015111_44867
319	NM_033212_58269	396	NM_001284401_26422	473	NM_001242898_20986	550	NM_015225_45095
320	NM_033426_58519	397	NM_001136197_11772	474	NM_002749_31537	551	NM_014907_44437
321	NM_001282306_25488	398	NM_001135176_11346	475	NM_181646_66960	552	NM_006293_39201
322	NM_003737_33737	399	NM_178507_66474	476	NM_001267595_23381	553	NM_153478_64120
323	NM_001276717_24353	400	NM_001135655_11469	477	NM_182529_67337	554	NM_153638_64195
324	NM_021026_51842	401	NM_019593_50358	478	NM_000296_665	555	NM_015680_45884
325	NM_001099408_8539	402	NM_006806_40314	479	NM_001164760_15191	556	NM_001142675_12452
326	NM_016006_46286	403	NM_000887_1957	480	NM_015446_45510	557	NM_002419_30793
327	NM_001134338_11027	404	NM_017635_47853	481	NM_006946_40615	558	NM_003601_33450
328	NM_001719_29189	405	NM_001126181_9883	482	NM_020753_51321	559	NM_001243271_21178
329	NM_001136566_11951	406	NM_005913_38392	483	NM_003815_33908	560	NM_002391_30734
330	NM_018143_48851	407	NM_025108_55124	484	NM_170776_64505	561	NM_001291284_28185
331	NM_006832_40382	408	NM_018960_49992	485	NM_173565_65089	562	NM_006297_39209
332	NM_174938_65551	409	NM_001010940_4356	486	NM_182612_67468	563	NM_001282741_25956
333	NM_024759_54608	410	NM_101395_59817	487	NM_001139518_12050	564	NM_014351_43329
334	NM_173511_64967	411	NM_201544_69207	488	NM_001037582_5994	565	NM_020443_50984
335	NM_014248_43120	412	NM_182642_67505	489	NM_007277_41256	566	NM_004311_34907
336	NM_006955_40639	413	NM_153371_64053	490	NM_078626_59360	567	NM_003677_33608
337	NM_001077269_7069	414	NM_002903_31889	491	NM_001130674_10784	568	NM_001127665_10163
338	NM_017761_48081	415	NM_001201481_19584	492	NM_001104589_9075	569	NM_080881_59796
339	NM_012417_42124	416	NM_054110_59183	493	NM_033036_57990	570	NM_001177693_17091
340	NM_001129765_10502	417	NM_020734_51278	494	NM_001113561_9496	571	NM_001193466_18083
341	NM_005915_38398	418	NM_003411_33033	495	NM_080592_59464	572	NM_005242_36902
342	NM_001662_29057	419	NM_194291_67933	496	NM_001289773_27797	573	NM_017617_47817
343	NM_001286351_26677	420	NM_013275_42383	497	NM_001083111_7897	574	NM_005361_37189
344	NM_003592_33428	421	NM_019021_50112	498	NM_001077181_7041	575	NM_030806_55660
345	NM_003683_33623	422	NM_004923_36183	499	NM_016653_47440	576	NM_001114974_9626
346	NM_022124_52859	423	NM_001042590_6750	500	NM_001278650_25039	577	NM_001009939_4172

347	NM_198495_68456	424	NM_001802_29387	501	NM_139245_61121	578	NM_022970_53542
348	NM_022167_52972	425	NM_001042454_6659	502	NM_001013698_4764	579	NM_001025300_5409
349	NM_005892_38348	426	NM_003948_34198	503	NM_182614_67469	580	NM_001285829_26516
350	NM_006766_40227	427	NM_024864_54824	504	NM_017777_48112	581	NM_002733_31495
351	NM_012223_41707	428	NM_016076_46442	505	NM_001170699_16170	582	NM_001134773_11189
352	NM_006548_39760	429	NM_003642_33527	506	NM_001134876_11221	583	NM_002213_30347
353	NM_207426_70072	430	NM_017514_47654	507	NM_001420_28605	584	NM_001029882_5484
354	NM_001134407_11054	431	NM_198239_68226	508	NM_006873_40471	585	NM_001199852_19398
355	NM_021005_51801	432	NM_014952_44540	509	NM_014907_44439	586	NM_001024212_5211
356	NM_001242613_20764	433	NM_001271852_24025	510	NM_145235_61928	587	NM_001127212_9943
357	NM_001441_28648	434	NM_001110199_9258	511	NM_003096_32349	588	NM_018026_48598
358	NM_001024858_5311	435	NM_001010897_4295	512	NM_032800_57608	589	NM_015114_44878
359	NM_023933_53687	436	NM_018231_49035	513	NM_138799_60869	590	NM_001243288_21190
360	NM_022458_53129	437	NM_001207009_20408	514	NM_002334_30619	591	NM_001272051_24160
361	NM_001199747_19311	438	NM_001256024_22022	515	NM_001143836_12695	592	NM_001080123_7342
362	NM_001172412_16578	439	NM_001010846_4203	516	NM_017414_47518	593	NM_001039613_6186
363	NM_001252076_21719	440	NM_153230_63857	517	NM_030792_55637	594	NM_032810_57639
364	NM_001289145_27713	441	NM_152744_63481	518	NM_002748_31534	595	NM_001035_5846
365	NM_001135865_11590	442	NM_001098484_8252	519	NM_001276320_24249	596	NM_001206998_20395
366	NM_147147_62310	443	NM_001093772_8135	520	NM_001012643_4541	597	NM_021129_52008
367	NM_013296_42417	444	NM_001256657_22431	521	NM_001528_28821	598	NM_001286767_27011
368	NM_153280_63941	445	NM_032265_56735	522	NM_138970_60937	599	NM_001204871_20078
369	NM_001161368_14517	446	NM_001199323_19154	523	NM_001177984_17131	600	NM_001031672_5560
370	NM_178232_66297	447	NM_001166215_15501	524	NM_032641_57421	601	NM_001076675_7008
371	NM_021920_52517	448	NM_001243565_21299	525	NM_001134363_11034	602	NM_001199687_19281
372	NM_001114636_9610	449	NM_002360_30677	526	NM_001098509_8271	603	NM_001042590_6749
373	NM_001252231_21754	450	NM_002775_31600	527	NM_138983_60949	604	NM_001143943_12750
374	NM_001198719_18768	451	NM_001135086_11284	528	NM_007010_40741	605	NM_002720_31468
375	NM_018198_48956	452	NM_001145638_13664	529	NM_001100399_8762	606	NM_014699_44004
376	NM_004426_35142	453	NM_002061_29984	530	NM_006293_39202	607	NM_004577_35474
377	NM_021965_52625	454	NM_153266_63916	531	NM_001007533_3904	608	NM_003036_32204
378	NM_018250_49068	455	NM_021238_52234	532	NM_021077_51924	609	NM_001084392_8003
379	NM_006029_38635	456	NM_052850_58762	533	NM_004752_35843	610	NM_194455_68017
380	NM_001256163_22114	457	NM_001080483_7586	534	NM_014213_43045	611	NM_014334_43291
381	NM_138431_60552	458	NM_207380_69989	535	NM_001268_23454	612	NM_014862_44337
382	NM_001162422_14671	459	NM_003842_33973	536	NM_002196_30309	613	NM_001113363_9413
383	NM_001145210_13342	460	NM_001112_9355	537	NM_001169111_16065	614	NM_024122_53952
384	NM_002859_31788	461	NM_052870_58807	538	NM_001136271_11841	615	NM_033427_58522
385	NM_173560_65078	462	NM_003863_34016	539	NM_015503_45608	616	NM_001256235_22140

rank	sgRNA ID	rank	sgRNA ID	rank	sgRNA ID	rank	sgRNA ID
617	NM_001199580_19236	694	NM_006998_40715	771	NM_016369_46967	848	NM_024587_54278
618	NM_023072_53615	695	NM_022802_53425	772	NM_145001_61703	849	NM_018363_49294
619	NM_015415_45449	696	NM_014480_43600	773	NM_018132_48826	850	NM_000717_1615
620	NM_001286464_26757	697	NM_001286440_26733	774	NM_001130100_10685	851	NM_003271_32720
621	NM_002467_30900	698	NM_178310_66316	775	NM_001252391_21792	852	NM_012101_41490
622	NM_183004_67749	699	NM_000695_1561	776	NM_014957_44554	853	NM_015898_46067
623	NM_207355_69941	700	NM_018419_49412	777	NM_001206997_20392	854	NM_001141936_12064
624	NM_003705_33666	701	NM_001160233_14438	778	NM_152365_62732	855	NM_014398_43428
625	NM_001130674_10785	702	NM_000702_1581	779	NM_001079839_7285	856	NM_001206541_20192
626	NM_001206710_20247	703	NM_018389_49353	780	NM_015696_45921	857	NM_031894_56233
627	NM_003493_33190	704	NM_001142275_12103	781	NM_020812_51447	858	NM_138395_60484
628	NM_001969_29777	705	NM_000031_41	782	NM_177538_66082	859	NM_001290204_28002
629	NM_023037_53597	706	NM_001246_21612	783	NM_052988_59018	860	NM_001167_15711
630	NM_006534_39726	707	NM_000095_193	784	NM_001142281_12109	861	NM_001134451_11085
631	NM_001098722_8392	708	NM_023016_53577	785	NM_001289121_27695	862	NM_001279351_25159
632	NM_080606_59487	709	NM_001166694_15698	786	NM_001127692_10177	863	NM_001018072_5132
633	NM_003862_34011	710	NM_003628_33495	787	NM_022757_53358	864	NM_153254_63892
634	NM_001256853_22575	711	NM_000504_1167	788	NM_001025591_5420	865	NM_012461_42220
635	NM_032120_56519	712	NM_024596_54296	789	NM_006456_39566	866	NM_032822_57662
636	NM_001004757_3243	713	NM_002062_29985	790	NM_001040458_6513	867	NM_001024466_5241
637	NM_005313_37074	714	NM_033027_57967	791	NM_001082579_7874	868	NM_080628_59532
638	NM_001267043_23324	715	NM_031423_56068	792	NM_006577_39829	869	NM_001278138_24572
639	NM_033518_58618	716	NM_001166239_15510	793	NM_002699_31419	870	NM_144567_61233
640	NM_003216_32600	717	NM_001282391_25554	794	NM_001163315_14771	871	NM_012333_41953
641	NM_015423_45468	718	NM_001098805_8416	795	NM_001205319_20171	872	NM_145644_62112
642	NM_032305_56810	719	NM_001282449_25632	796	NM_003815_33909	873	NM_002531_31059
643	NM_017691_47954	720	NM_001077621_7135	797	NM_001171039_16292	874	NM_001100389_8745
644	NM_001184743_17365	721	NM_024083_53862	798	NM_032598_57358	875	NM_001289061_27662
645	NM_015348_45327	722	NM_001164579_15109	799	NM_183419_67868	876	NM_001284400_26417
646	NM_001253699_21848	723	NM_001163474_14805	800	NM_001493_28738	877	NM_005003_36378
647	NM_173567_65096	724	NM_001204082_19804	801	NM_153357_64014	878	NM_001289145_27714
648	NM_001287748_27345	725	NM_133369_60079	802	NM_001130136_10703	879	NM_001160333_14470
649	NM_032731_57509	726	NM_022829_53456	803	NM_001006117_3755	880	NM_003720_33698
650	NM_152666_63338	727	NM_001136020_11659	804	NM_003776_33820	881	NM_006005_38595
651	NM_012289_41850	728	NM_004804_35949	805	NM_013234_42281	882	NM_014755_44144
652	NM_001278710_25089	729	NM_021632_52341	806	NM_000698_1569	883	NM_004055_34383
653	NM_001258248_22922	730	NM_001145208_13338	807	NM_058181_59276	884	NM_001252120_21732
654	NM_001206994_20384	731	NM_003704_33661	808	NM_001033581_5775	885	NM_001134709_11174

655	NM_022977_53546	732	NM_032783_57570	809	NM_005967_38508	886	NM_001289413_27773
656	NM_001290557_28124	733	NM_001282534_25744	810	NM_032420_57028	887	NM_001009894_4157
657	NM_021977_52647	734	NM_024522_54161	811	NM_014317_43253	888	NM_001201334_19527
658	NM_153029_63763	735	NM_001199954_19479	812	NM_004215_34721	889	NM_007226_41149
659	NM_006577_39830	736	NM_032133_56540	813	NM_033071_58050	890	NM_015221_45089
660	NM_001136180_11759	737	NM_001135208_11370	814	NM_016009_46292	891	NM_001267036_23312
661	NM_001287253_27200	738	NM_001013742_4787	815	NM_001284206_26231	892	NM_032827_57676
662	NM_001416_28592	739	NM_198082_68105	816	NM_001024957_5329	893	NM_173050_64740
663	NM_001034914_5840	740	NM_001004311_2844	817	NM_002690_31399	894	NM_001290260_28059
664	NM_002346_30648	741	NM_001111032_9298	818	NM_001286839_27082	895	NM_024875_54846
665	NM_001142352_12193	742	NM_005334_37129	819	NM_017672_47921	896	NM_001190799_17781
666	NM_018929_49911	743	NM_001100817_8820	820	NM_001244584_21489	897	NM_001257342_22745
667	NM_001242898_20987	744	NM_022912_53523	821	NM_017514_47653	898	NM_138328_60363
668	NM_001145399_13512	745	NM_001098403_8238	822	NM_001280557_25184	899	NM_004521_35341
669	NM_001160148_14404	746	NM_182488_67248	823	NM_152996_63713	900	NM_020179_50617
670	NM_207661_70152	747	NM_001184974_17485	824	NM_003647_33542	901	NM_014159_42950
671	NM_031268_55930	748	NM_018928_49910	825	NM_001145139_13268	902	NM_016231_46716
672	NM_024014_53733	749	NM_001080541_7726	826	NM_198482_68421	903	NM_007068_40865
673	NM_022463_53139	750	NM_001932_29687	827	NM_001080484_7590	904	NM_005206_36823
674	NM_018163_48892	751	NM_001287240_27189	828	NM_022566_53241	905	NM_014726_44075
675	NM_018475_49518	752	NM_001042631_6768	829	NM_021249_52263	906	NM_004092_34461
676	NM_001164385_15003	753	NM_006136_38843	830	NM_014410_43455	907	NM_001164811_15223
677	NM_019612_50391	754	NM_018226_49022	831	NM_019112_50313	908	NM_133445_60117
678	NM_005539_37595	755	NM_144568_61237	832	NM_018280_49128	909	NM_001290202_27997
679	NM_005552_37617	756	NM_024309_53987	833	NM_001281513_25287	910	NM_001080406_7400
680	NM_007041_40814	757	NM_015720_45967	834	NM_001042391_6591	911	NM_015230_45103
681	NM_001991_29834	758	NM_001172673_16689	835	NM_080391_59401	912	NM_001278503_24873
682	NM_014246_43112	759	NM_004427_35145	836	NM_005486_37467	913	NM_173570_65103
683	NM_001099650_8590	760	NM_004928_36198	837	NM_001168393_15996	914	NM_052905_58874
684	NM_001128228_10335	761	NM_001005368_3547	838	NM_003211_32585	915	NM_001271518_23834
685	NM_021130_52013	762	NM_024686_54485	839	NM_145115_61835	916	NM_001278461_24841
686	NM_001267616_23401	763	NM_130811_59951	840	NM_001080488_7600	917	NM_001159293_14213
687	NM_001256421_22276	764	NM_005197_36805	841	NM_002118_30112	918	NM_004106_34493
688	NM_001256526_22339	765	NM_022121_52854	842	NM_001077441_7098	919	NM_001202515_19720
689	NM_001193635_18203	766	NM_022571_53253	843	NM_018263_49093	920	NM_003841_33969
690	NM_015275_45189	767	NM_001288824_27561	844	NM_205767_69550	921	NM_001127487_10086
691	NM_016516_47189	768	NM_017864_48298	845	NM_000053_92	922	NM_001017969_5046
692	NM_025069_55079	769	NM_001243731_21347	846	NM_001166304_15582	923	NM_006043_38674
693	NM_198572_68588	770	NM_024980_54995	847	NM_001142676_12455	924	NM_003978_34265

rank	sgRNA ID	rank	sgRNA ID	rank	sgRNA ID	rank	sgRNA ID
925	NM_003492_33188	951	NM_020354_50821	977	NM_024681_54472	1003	NM_130849_59980
926	NM_014747_44124	952	NM_024121_53949	978	NM_005493_37478	1004	NM_145167_61846
927	NM_001130_10572	953	NM_001018008_5099	979	NM_001284424_26441	1005	NM_002900_31880
928	NM_138370_60440	954	NM_001276464_24317	980	NM_001035235_5866	1006	NM_001172702_16733
929	NM_014589_43758	955	NM_001243895_21432	981	NM_014293_43204	1007	NM_152470_62953
930	NM_052877_58827	956	NM_001253855_21914	982	NM_032458_57115	1008	NM_001943_29714
931	NM_001080464_7532	957	NM_003741_33744	983	NM_006654_39999	1009	NM_175710_65707
932	NM_199141_68905	958	NM_004635_35599	984	NM_022731_53301	1010	NM_006990_40698
933	NM_001172813_16783	959	NM_001101339_8875	985	NM_001190737_17753	1011	NM_000232_515
934	NM_001113493_9456	960	NM_001159390_14232	986	NM_004260_34804	1012	NM_013319_42458
935	NM_001168325_15941	961	NM_006134_38839	987	NM_013341_42503	1013	NM_003059_32265
936	NM_173472_64880	962	NM_001286756_27001	988	NM_001173552_16892	1014	NM_001145201_13330
937	NM_012447_42180	963	NM_001198807_18824	989	NM_006653_39996	1015	NM_019029_50133
938	NM_178124_66223	964	NM_001271618_23861	990	NM_022787_53416	1016	NM_021964_52621
939	NM_001124758_9819	965	NM_001098498_8260	991	NM_001288720_27490	1017	NM_016565_47285
940	NM_000441_1027	966	NM_014424_43479	992	NM_021630_52339	1018	NM_002980_32058
941	NM_001034838_5827	967	NM_004499_35304	993	NM_021705_52384	1019	NM_138734_60788
942	NM_024809_54724	968	NM_020666_51150	994	NM_001010846_4204	1020	NM_001035254_5868
943	NM_024430_54100	969	NM_001134778_11200	995	NM_001164773_15206	1021	NM_001144_12845
944	NM_000367_834	970	NM_022896_53491	996	NM_001204065_19792	1022	NM_001162505_14694
945	NM_000665_1488	971	NM_032383_56977	997	NM_015904_46076	1023	NM_001201477_19582
946	NM_138499_60669	972	NM_002726_31478	998	NM_001130929_10917	1024	NM_001290293_28081
947	NM_001204255_19908	973	NM_001122870_9747	999	NM_001253801_21888		
948	NM_001256114_22079	974	NM_001278677_25062	1000	NM_001258354_23010		
949	NM_022571_53255	975	NM_001039707_6234	1001	NM_004857_36062		
950	NM_001288962_27591	976	NM_022062_52747	1002	NM_001127598_10117		

Publications

1. **Tong Z**, Cao C, Rao M, Lu J, Tan J. (2015) Potential Cell Source for Cell-Based Therapy and Tissue Engineering Applications: Urine-Derived Stem Cells. Journal of Biomaterials and Tissue Engineering 5(2)

2. Sathe A, Chalaud G, Oppolzer I, Wong KY, von Busch M, Schmid SC, **Tong Z**, Retz M, Gschwend JE, Schulz WA, Nawroth R. (2018) Parallel PI3K, AKT and mTOR inhibition is required to control feedback loops that limit tumor therapy. PLoS One. 2018 Jan 22;13(1)